Sapienza University of Rome

PhD Program in Molecular Medicine
Molecular Medicine Section

Biomolecular characterization of metastatic medulloblastoma and study of telomere lengthening control

CANDIDATE
Dott. Simone Minasi

TUTOR
Prof.ssa Francesca Romana Buttarelli

XXX CYCLE

A.A. 2017

SUMMARY:

Introductory note

From the research conducted in the three years of PhD, the following articles, abstract and presentations were published in national and international pediatric Neuro-oncology congresses:

- **FSTL5 expression is a marker of Group C metastatic medulloblastomas.**
  Authors: C. Baldi, **S. Minasi**, F. Gianno, M. Massimino, F. Giangaspero, and F.R. Buttarelli.
  Abstract - Poster "British Neuro Oncology Society (BNOS) Conference Report 2014" Liverpool; **P-43**.

- **Distribution and prognostic impact of molecular subgroups in a homogeneously treated series of metastatic medulloblastoma.**
  Authors: M. Massimino, F.R. Buttarelli, C. Baldi, **S. Minasi**, M. Antonelli, F. Giangaspero.
  Abstract - Poster 47th Congress of International Society of Pediatric Oncology (SIOP) 2015, Cape Town; **P-158**.

- **Distribution and prognostic impact of molecular subgroups in a homogeneously treated series of metastatic medulloblastoma.**
  Authors: F.R. Buttarelli, F. Giangaspero, **S. Minasi**, M. Antonelli, M. Massimino.
  Abstract - Poster "International Symposium on Pediatric Neuro-Oncology (ISPNO 2016)" Leeds; **MB-76**.

- **Brafv600e and Ctbn1 Mutational Study in Rathke's Cleft Cysts.**
  Authors: Antonelli M, Badiali M, Moi L, Arcella A, Buttarelli FR, **S. Minasi** and Giangaspero F.
  Article published on September 05, 2016; J Clin Exp Pathol 2016, 6:5; **doi: 10.4172/2161-0681.1000291**.

Furthermore, during the three years of PhD, I was declared the winner of the following research fellowship on the project:

- **Study of tumor biomarkers for molecular characterization of pediatric medulloblastomas.**
  "Sapienza University of Rome", Department of Paediatrics and Child Neurology; Scientific Director Professor Anna Clerico.

INTRODUCTION

Pediatric brain tumors

Central Nervous System (SNC) tumors are the principle cause of death for children and adolescents. Central Brain Tumor Registry of the United States (CBTRUS) data reported that most of pediatric brain tumors are situated in hemisphere (18%), followed by cerebellum (15%), brainstem (11%) e ventricles (6%). Carcinogenesis is a multistep process in which epigenetic changes and genetic alterations accumulate in the genomes of cancer cells. Few molecular hallmarks and signaling abnormalities have been identified as drivers for most aggressive tumors.

Pediatric brain tumors (PBT), comprising multiple separate pathological entities, are the most common group of solid cancers in children (Mangerel et al., 2014). Recent discoveries using next-generation genomic platforms have uncovered substantial molecular heterogeneity even amongst PBTs with the same histological classification, like subgroups of medulloblastoma (De Braganca et al., 2013; Kool et al., 2008), glioma (Kim JH et al., 2013), and ependymoma (Mack et al., 2014; Parker et al., 2014).

Malignant gliomas represent 55% of CNS tumors in childhood and the 71% of malignant CNS tumors in adults; pediatric high-grade gliomas (pHGG) are histologically similar to the adult counterpart, but show some differences at molecular level.

Although curative therapy options are still absent and long-term survivors are an exception in adults as well as in children (Reifenberger et al., 2014*)*, infants (< 3 years of age) with high-grade gliomas (iHGG) appear to have a better clinical outcome (Antonelli et el., 2010; Batra et al. 2014, Karremann et al., 2013; Merchant et al., 2010*)*. Pediatric high grade gliomas (pHGG) are classified and graded according to histological criteria (oligodendroglioma, oligoastrocytoma, astrocytoma, and glioblastoma; grade II to IV). Although histopathologic classification is well established and is the basis of the World Health Organization (WHO) classification of CNS tumors (Louis et al., 2007), it suffers from high intra- and inter- variability. Recent molecular characterization studies have related genetic, gene expression, and DNA methylation signatures with prognosis (Noushmehr et al., 2010; Sturm et al., 2012).

In cerebellum medulloblastomas arise from the external granular layer, correspond to grade IV WHO, and often occur with leptomeningeal dissemination at the onset. Although medulloblastoma is the most common malignant brain tumor of childhood, the identity of molecules that are useful therapeutic targets in medulloblastoma is largely unknown due to the lack of fundamental knowledge on the molecular pathogenesis of the disease. Within the last few years it became clear that medulloblastoma is a very heterogeneous disease comprising at least four molecular subgroups (WNT, SHH, Group 3 and Group 4), associated with different outcomes (Northcott et al., 2011; Taylor et al., 2012; Ramaswamy et al., 2016).

Molecular subgrouping of medulloblastomas

Medulloblastoma (MDB), the most frequent malignant brain tumor in children, is a clinically and biologically heterogeneous disease. The prognostic system based on clinical parameters such as patient age, extent of surgical resection, metastatic spread and histopathological variants is commonly used in clinical practice (Ellison et al., 2010; Korshunov et al., 2012). Approximately 10% to 15% of patients die from disease within 2 years after diagnosis, whereas approximately 60% of patients can now be cured (Massimino et al., 2012; Ramaswamy et al., 2016; Van Bueren et al., 2016). Recent studies of gene expression profiles revealed distinct molecular subgroups with different biological features (Kool et al., 2012; Ramaswamy et al., 2016; Taylor et al., 2012); the current consensus predicts the existence of four subgroups: SHH, WNT, group 3 and group 4, associated with different outcome of patients (Fattet et., 2009; Kool et al., 2008; Northcott et al., 2011; Northcott et al., 2012a; Northcott et al., 2012b; Ramaswamy et al., 2016; Remke et al., 2011b; Robinson et al 2012; Taylor et al., 2012). The group WNT is associated with nuclear translocation of β-catenin, mutations in exon 3 of CTNNB1 and monosomy of chromosome 6. The outcome is excellent, with a survival rate over 90% (Ellison et al., 2011b; Ellison et al., 2005; Fattet et al., 2009; Ramaswamy et al., 2016). The SHH group is associated with somatic mutations of the genes SMO, PTCH and SUFU, triple immuno-positivity for GAB1, YAP1 and Filamin A, TP53 mutations, amplification of MYCN and GLI2, deletion of chromosome 9q and 10q and duplication of chromosome 3q (Ellison et al., 2011b; Korshunov et al., 2012; Ramaswamy et al., 2016; Taylor et al., 2012). Tumors in group 3 are characterized by the loss of chromosomes 10q and 5q, duplication of chromosome 1q, NPR3 and OTX2 high expression and recurrent MYC amplification (Ramaswamy et al., 2016; Robinson et al., 2012; Taylor et al., 2012). Within group 4 MDB, tumors are characterized by MYCN amplification, immuno-positivity for KCNA1 and OTX2, loss of the X chromosome in female subjects and isochromosome 17q, also shared by the group 3 (Ellison et al., 2011a; Ellison et al., 2011b; Ellison et al., 2005; Korshunov et al., 2012; Ramaswamy et al., 2016; Robinson et al., 2012; Taylor et al., 2012); for group 3 and 4, there is no evidence of any alteration in a specific pathway.

Medulloblastomas can disseminate through the cerebrospinal fluid in the leptomeningeal space to coat the brain and spinal cord. Metastasis arise from a restricted

sub-clone of the primary tumor, in which genetic events make neoplastic cells able to metastasize, through a process of clonal selection (Wu et al., 2012).

Across several biologically informed cohorts of pediatric MDB, metastatic dissemination was considered as a marker of poor prognosis (Lannering et al., 2012). Various studies indicated molecular subgrouping correlation with prognostic stratification of pediatric patients, but some survival information remain unknown for MDB with metastatic spread at diagnosis. Recent study confirmed the relevance of subgroup status and biologic parameters (WNT/MYCC/MYCN status) in a homogeneous prospective trial population of 121 metastatic MDB (Van Bueren et al., 2016); data evidenced a favourable risk group (metastatic WNT-patients), a high-risk group (group 3 with MYC or MYCN amplification), and a large group of intermediate-risk patients (Van Bueren et al., 2016).

Risk groups were defined based on current survival rates: low risk (>90% survival), standard risk (75-90% survival), high risk (75-50% survival) and very high risk (<50% survival) (Ramaswamy et al., 2016). Group 3 are frequently metastatic (>50%) and overall outcome is worse compared to the other subgroups (Ramaswamy et al., 2013); group 3 cases with metastasis at the onset have been identified as being very high risk (Ramaswamy et al., 2016; Shih et al., 2014; Van Bueren et al., 2016). Approximately 30% of group 4 medulloblastomas are metastatic at diagnosis; metastatic cases of group SHH and group 4 were considered high risk patients (**Fig. 1**) (Ramaswamy et al., 2013; Ramaswamy et al., 2016; Van Bueren et al., 2016). The low incidence of metastatic dissemination in WNT (<5%) medulloblastomas precludes any recommendation, and their risk stratification remains indeterminate (Ramaswamy et al., 2016). However, recent work showed the prognostic role of WNT activation in a cohort of patients with metastatic disease and highlighted that four patients with metastatic WNT-activated medulloblastoma survived without relapse, indicating that WNT metastatic MDB may be treated successfully by less intensive treatment regimens (standard risk protocol) because they might be overtreated by current high-risk regimens (Van Bueren et al., 2016).

In conclusion, only one published work (Van Bueren et al., 2016) analyzed medulloblastomas with metastasis at the onset separately from primary medulloblastoma; in fact, the percentage of metastatic cases in most of the studies did not exceed 30% and were not analyzed independently from the non-metastatic counterpart. We evaluated molecular biomarkers and subgroups in a large cohort of

pediatric patients with leptomeningeal dissemination at the onset, in order to define risk classes and to elucidate relevant aspects of the metastatic disease.

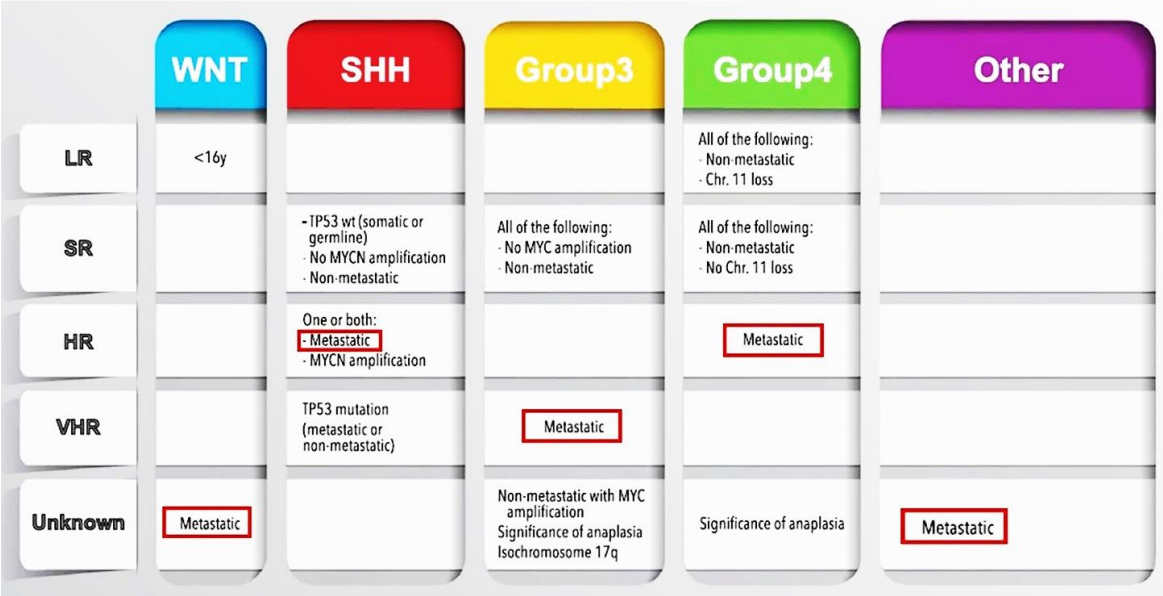

Fig. 1: Current proposed risk stratification by Ramaswamy and colleagues for childhood medulloblastoma with metastasis at diagnosis. *LR* low risk, *SR* standard risk, *HR* high risk, *VHR* very high risk (from: Ramaswamy et al., 2016).

Follistatin-like 5

Follistatin-like 5 (FSTL5), a member of the follistatin family of genes, encodes a secretory glycoprotein. Previous study revealed that it might play a role in MDB; FSTL5 was over-expressed in group 3 and high-risk group 4 tumors and was significantly associated with reduced progression-free and overall survival across all disease variants; a lower FSTL5 expression characterized SHH and WNT group and correlated with a longer outcome (**Fig. 2**) (Gilbertson et al., 2011; Northcott et al., 2012a; Northcott et al., 2012b; Remke et al., 2011a). The current findings conclude that FSTL5 can be a reliable prognostic marker for MDB.

Recent study examined FSTL5 expression pattern in 117 hepatocellular carcinoma (HCC) tissue samples. The results of immune-histochemical staining and further clinicopathological analysis showed that FSTL5 expression level is closely correlated with tumor size, TNM stage, local infiltration and patient prognosis (Zhang et al., 2015). However, its clinical significances, biological functions and molecular mechanisms in cancer development are poorly understood.

FSTL5 gene encode a calcium ion (Ca^{2+}) binding domain; calcium-binding proteins participate in calcium cell signalling pathways by binding to Ca^{2+}. The dysregulation of Ca^{2+} homeostasis in cancer cells has been suggested as an important event in driving the expression of the malignant phenotypes, such as proliferation, migration, invasion, neo-angiogenesis and metastasis (Yang et al., 2010; Yih-Fung et al., 2013). Recent publication showed that elevated extra-cellular Ca^{2+} activated the calcium-sensing receptor (CaSR), a widely expressed homodimeric G-protein involved in promoting migration, brain development, stem-cell engraftment, wound healing, tumor growth and metastasis (Tharmalingam et al., 2016).

On the basis of the knowledge about pathways involved in the processes of invasion, metastasis and cell survival, we evaluated the FSTL5 gene expression levels and prognostic value in our cohort of metastatic medulloblastomas at the onset.

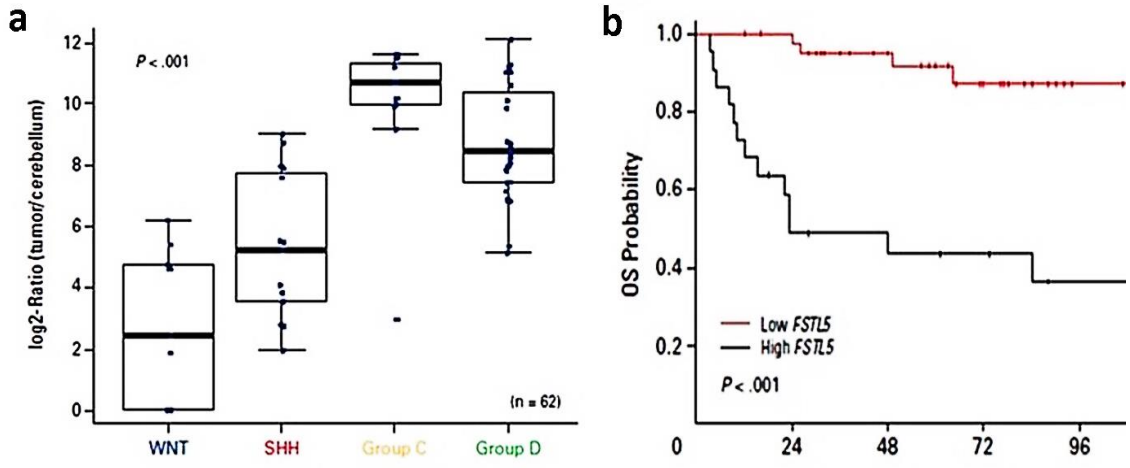

Fig. 2: Expression of follistatin-like 5 (FSTL5) transcripts derived from transcriptome analysis of primary medulloblastoma, grouped according to molecular disease variants (a). Kaplan-Meier plot of estimated OS time distributions according to FSTL5 mRNA (b) (from: Remke et al., 2011a).

Control of Telomeres lengthening and senescence escape

Cell immortalization has been considered for a long time as a classic hallmark of cancer cells. Telomeres are nucleoprotein complexes at the ends of eukaryotic chromosomes consisting of several repeats of the DNA sequence 5′-TTAGGG-3′, and contain no gene-coding information (Oganasian et al., 2009). The main function of telomeres is to preserve chromosome integrity and genome stability by preventing loss of genetic information which occurs due to lagging-strand shortening during DNA replication (Rubtsova et al., 2012). At each cell division, the telomeric DNA is diminished and telomeres become progressively shorter; eventually, this loss leads to a stop in cell division that forces cell senescence or cell death. Cells which are unable to maintain their telomeres undergo senescence and apoptosis; therefore, to maintain replicative ability, a telomere maintenance pathway must be activated by cancer cells (Ceccarelli et al., 2016; Mangerel et al., 2014).

Telomere length maintenance is required for tumor self-renewal and is activated ubiquitously in most malignant cancers. There are two major pathways that cells use to maintain telomere length; they either reactivate telomerase, a ribonucleoprotein polymerase which elongates telomeres by adding hexameric 5′-TTAGGG-3′ tandem repeats to the chromosomal ends, or take advantage of a non-telomerase-dependent mechanism, known as Alternative Lengthening of Telomeres (ALT) (Castelo-Branco et al., 2011; Ceccarelli et al., 2016; Cesare et al., 2010; Koelsche et al., 2013; Mangerel et al., 2014).

Telomerase has been found to be critically important for the maintenance of tumor-initiating cells, which are chemo-resistant cells able to repopulate the tumor and driver of recurrence (Marian et al., 2010). Telomeres are maintained in most cancers by telomerase reactivation, but a subset of tumors utilize alternative lengthening of telomeres to sustain self-renewal capacity (Castelo-Branco et al., 2011; Ceccarelli et al., 2016).

The telomerase complex comprises several components, but the telomerase reverse transcriptase catalytic subunit (TERT) (Cifuentes-Rojas et al., 2012; Montanaro et al., 2008; Nandakumar et al., 2013) is the only component necessary to restore the activity of the telomerase complex.

Recently, activating mutations in the TERT promoter were uncovered in melanoma (Horn et al., 2013) and other tumors, including several brain tumors (Ceccarelli et al.,

2016; Koelsche et al., 2013; Mangerel et al., 2014). The TERT gene is located on chromosome 5 and includes 16 exons that span a 35-kb region. The core promoter of TERT includes 630 base pairs upstream of the start site, was in a GC-rich region and contains transcript sites/consensus for transcription elements, indicating a high level of regulation by multiple factors at transcriptional and/or post-transcriptional level (Cifuentes-Rojas C et al., 2012).

Hot spot mutations in the promoter region of TERT result in an upregulation of telomerase complex activity and thus constitute a relevant mechanism for the maintenance of telomere length and the immortalization of tumor cells. Among CNS tumors, gliomas are those displaying by far the highest frequency of TERT mutations, but these promoter mutations are rarer in pediatric CNS tumors (Ceccarelli et al., 2016; Koelsche et al., 2013); in pediatric medulloblastomas, TERT promoter mutations are mainly detected in tumors of the group of older patients and are associated with sonic hedgehog and WNT mutations (Remke, Ramaswamy et al., 2013). TERT promoter mutations are rare in pediatric tumors of the CNS; these findings are consistent with the fact that the cells, from which pediatric CNS tumors are thought to originate, still have activated telomerase which obviates the need for activation of TERT through promoter mutation.

Within adult gliomas, the percentage of cases with TERT promoter mutations differs according to the histopathological type of tumors. TERT promoter mutations are detected in most cases of glioblastoma multiforme (GBM), in contrast to astrocytoma and ependymoma, in which only a small percentage of the tumors harbors such mutations (Killela et al., 2013; Koelsche et al., 2013). The low frequency of TERT promoter mutations and telomerase activity in grades II and III astrocytomas can be explained by the high prevalence of ATRX mutations, one of the most frequent mutations in this type of gliomas (Jiao et al., 2012). It is known that ATRX mutations trigger ALT in astrocytoma cells and it has been shown that this alternative mechanism is frequently activated in astrocytomas, allowing telomere maintenance without the need for telomerase reactivation (Henson et al., 2005). In line with this, the frequency of TERT promoter mutations in secondary GBMs (that arise from the progression of lower grade astrocytomas) is considerably lower than in primary GBMs, that appear de novo (Nonoguchi et al., 2013).

Furthermore, recent works about DNA methylation study at the TERT promoter identified a subset of five CpG sites (henceforth, upstream of the transcription start site

[UTSS]) that was hyper-methylated in all malignant paediatric brain tumours but not in normal tissues, increasing TERT expression and elongation of telomeres by reactivation of telomerase (Castelo-Branco et al., 2013). TERT promoter region UTSS was shown in Figure 3 (**Fig. 3**). In paediatric brain tumours, UTSS hyper-methylation is associated with tumour progression and poor prognosis. This region is easy to amplify, and the assay to establish hypermethylation can be done on most tissues in most clinical laboratories. Therefore, the UTSS region is a potentially accessible biomarker for pediatric brain tumors (Castelo-Branco et al., 2013).

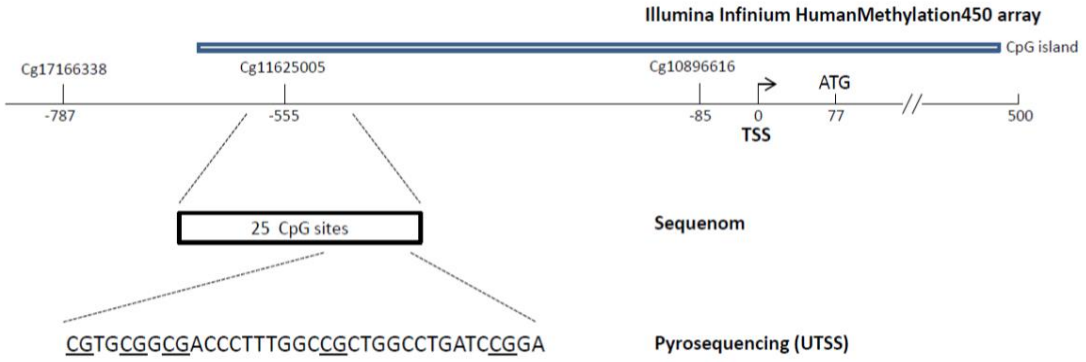

Fig. 3: The Illumina Infinium HumanMethylation450 array covers the area with the probes Cg17166338, Cg11625005 and Cg10896616. The amplified regions used for Sequenom and pyrosequencing (UTSS region) analyses are shown as open box and 36 bp sequence. Underlined are the 5 targeted CpG sites (from: Castelo-Branco et al., 2013).

Tumors which do not activate telomerase utilize the less well-defined alternative lengthening of telomeres (ALT) phenotype which maintains telomeres in a telomerase-independent manner, presumably by telomere-specific homologous recombination (Bechter et al., 2003; Mangerel et al., 2014; Nabetani et al., 2011). The molecular basis of activation of ALT are not yet fully known. It has been shown that during the replication-independent chromatin assembly, ATRX and DAXX proteins act together in the deposition and stabilization of histone H3.3 on DNA (**Fig. 4**).

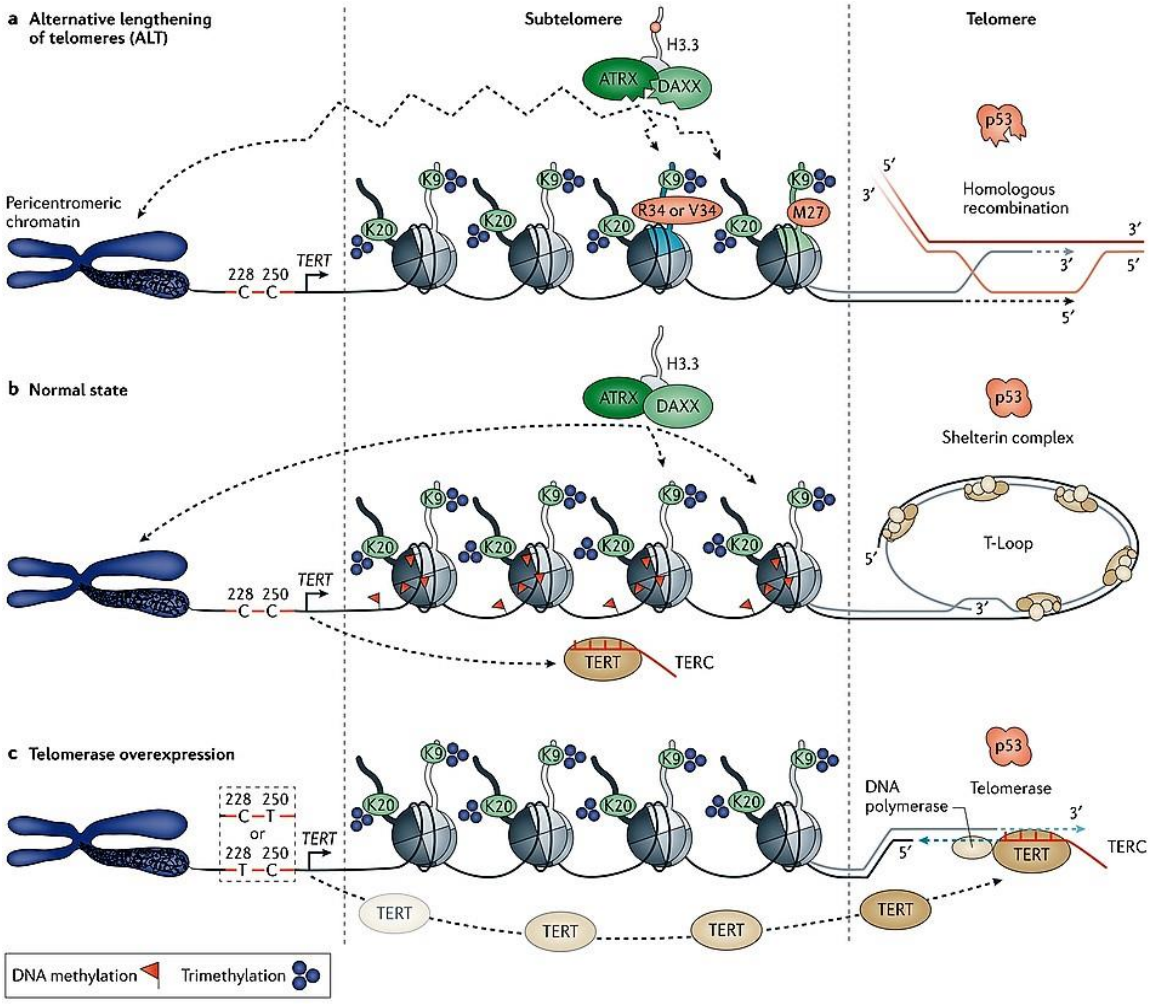

Fig. 4: Mechanism of telomere length maintenance by ALT (a) or telomerase reactivation (c). The normal state was shown in figure b (from: Sturm et al., 2014).

Next generation sequencing efforts have revealed a strong association of ATRX mutations in several adult tumors which exhibit ALT. ATRX is a protein involved in loading the histone 3 variant H3.3, the product of the H3f3a gene, at the telomeres, favouring formation of heterochromatin (Lovejoy et al., 2012; Schwartzentruber et al., 2012). As ALT occurs by homologous recombination, loss of a heterochromatic state at the telomeres is permissive for this recombination to occur (Episkopou et al. 2014; Mangerel et al., 2014).

Heaphy and colleagues observed the presence of ALT in brain tumors as medulloblastoma, schwannoma and glioblastoma, but its absence in all benign neoplasms and normal tissues (Ceccarelli et al., 2016; Heaphy, Subhawong et al., 2011; Mangerel et al., 2014). Later, they demonstrated that ATRX or DAXX mutations are

closely associated with the development of ALT in pancreatic endocrine tumors, whereas ATRX or H3.3 mutations lead to ALT phenotype in cancers of the central nervous system (Ceccarelli et al., 2016; Dong et al., 2012; Heaphy, de Wilde et al., 2011). Mutations in ATRX and H3.3 have been reported also in pediatric gliomas, correlated with ALT activation and increase of telomere length (**Fig. 5**) (Dong et al., 2012; Heaphy, de Wilde et al., 2011; Schwartzentruber J et al., 2012); however, their association and possible implication on the ALT phenotype in medulloblastomas were not so far investigated.

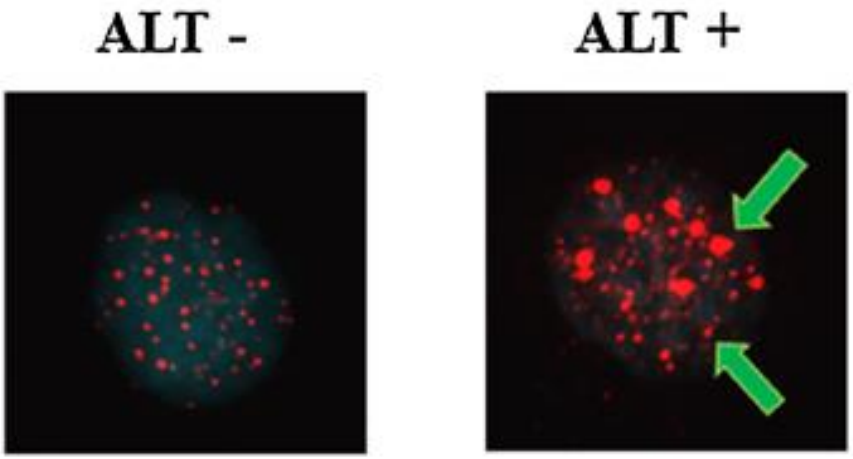

Fig. 5: ALT positive and negative cases in Telo-FISH. Red signals evidenced telomeric sequences (from: Mangerel et al., 2014).

ATRX, H3.3, TERT promoter mutations and UTSS methylation status could provide an explanation for the elongation of telomeres in most pediatric high-grade gliomas and metastatic medulloblastomas.

AIM OF THE STUDY

Medulloblastomas and high-grade gliomas are the most frequent brain tumors in children; nowadays, research in the field of pediatric neuro-oncology is focused on biomolecular characterization of pediatric tumors, in order to treat these cancers more adequately.

Medulloblastoma cells can disseminate through the cerebrospinal fluid in the leptomeningeal space; at present is not known which specific genetic/molecular alterations drive neoplastic cells to metastasize. Furthermore, in contrast to standard-risk non-metastatic medulloblastoma, no gold standard treatment has been defined for metastatic cases.

Our aim was to study specific molecular alterations involved in the processes of invasion, metastasis and cell survival in a series of 39 pediatric MDB with leptomeningeal dissemination at the onset and homogenously treated in a single institution, in order to define whether metastatic medulloblastomas are molecularly similar to non-metastatic ones, and whether could be identified genetic/molecular alterations involved in migration, invasiveness and malignancy of metastatic medulloblastoma cells.

We analyzed several subgroup biomarkers from FFPE samples and we correlated results to outcome of patients (OS and PFS), in order to evaluate the prognostic relevance of the molecular biomarkers and subgroups in our cohort of 39 metastatic MDB; in fact, previous studies in literature on molecular subgrouping analysis included only small amount of metastatic cases, not analyzed independently from the non-metastatic counterpart.

We analyzed FSTL5 gene expression to evaluate its significance as a high-risk biomarker associated with group 3/4 and bad outcome within our homogeneous cohort of pediatric patients with metastatic disease, since FSTL5 expression level was found to be closely correlated, in hepatocellular carcinoma as well as primary medulloblastoma, with tumor size, local infiltration and patient prognosis.

Furthermore, in the light of the knowledge on the cell survival and senescence escape, we evaluated the possible activation of a pathway controlling elongation of telomeres in metastatic medulloblastoma cells. We compared our cohort of 39 metastatic MDB with 56 pHGG, having different cellular origin but both with characteristics of high

malignancy, studying telomere length maintenance with telomerase reactivation or Alternative Lengthening of Telomeres (ALT); we analyzed H3.3, ATRX and DAXX, involved in ALT activation, along with the mutation and methylation status of TERT promoter.

Telomeres elongation has been reported in pediatric gliomas, correlated with ALT activation, however it was not previously investigated in medulloblastomas with leptomeningeal dissemination at diagnosis. For this reason, our goal was to analyze the activation of mechanisms involved in control of telomeres lengthening in metastatic cases, in order to figure out whether telomeres elongation could have a role in metastatic medulloblastoma cells.

Ongoing comprehensive genome analysis will undoubtedly identify more genes involved in the pathogenesis of medulloblastomas and gliomas. Among those genetic/epigenetic changes, we aim to identify novel molecular markers or therapeutic targets that could be used for clinical decision making or development of more effective treatment.

MATERIALS AND METHODS

Patients and tissue samples

Formalin-fixed paraffin embedded (FFPE) tissue specimens from 55 pediatric high-grade gliomas and 39 pediatric medulloblastomas with metastases at the onset were analyzed. All tumors were classified by four independent neuropathologists, according to the World Health Organization (WHO) classification of tumors of the central nervous system (Louis et al., 2007) using standard histological and immunohistochemical methods.

Fifty-five pediatric high-grade gliomas included 28 glioblastomas (GBM; WHO grade IV), 11 anaplastic astrocytomas (AA; WHO grade III), 6 pilocytic astrocytomas (AP; WHO grade III), 5 high grade ganglioneuronal and 4 primitive neuroectodermic tumors (PNET), retrieved from 36 Italian surgery Departments; also 1 oligoastrocytoma (OA; WHO grade II) was analyzed.

Medulloblastomas with metastasis at the onset were included in this study, were treated on the PNET4 /IT and were recruited from 1998 to 2014; age range was 3 to 21 years with median age of 12,5 years and an average follow-up of 155 months. The female/male ratio was 4/35. After complete surgical resection, patients received intensive sequential chemotherapy with high-dose methotrexate plus vincristine, high-dose etoposide, high-dose cyclophosphamide and high-dose carboplatin, followed by craniospinal hyperfractionated accelerated radiotherapy (HART) with posterior fossa boost and a post-radiant phase consisting of lomustine and vincristine for a total duration of one year or two myeloablative courses with high-dose thiotepa, chosen according to the entity of the pre-radiant chemotherapy response (Gandola et al., 2009).

Classical medulloblastomas were 30/39 (77%) cases of all tumors, followed by large/anaplastic (LC/A) histology with 7/39 (18%) and desmoplastic-nodular (D/N) with 2/39 (5%).

Immunohistochemistry (IHC)

Evaluation of protein expression was performed via immunohistochemistry. IHC was carried out by streptavidin–biotin–immunoperoxidase technique on 3-µm sections of FFPE samples. Slides were deparaffinized in xylene, and rehydrated through a graded series of ethanol dilutions, then incubated for 15 mins in 3% H2O2 in methanol to inhibit endogenous peroxidases. Tissue sections were then incubated in 10% normal rabbit serum to block nonspecific antibody binding. Antigen retrieval was performed in a microwave for 3×5 min at full power in sodium citrate buffer for all antibodies. Tissue sections were then incubated overnight (16-18 hrs) with the primary antibody. Sections were washed and incubated with biotinylated anti-polyvalent secondary antibody (Ultratek, Sciteck) for 20 min at room temperature. This was followed by incubation for 20 minutes with avidin–biotin peroxidase complex (Ultratek, Sciteck). Peroxidase activity was visualized by immersing sections in 0.03% 3.3′-diaminobenzidine–4HCl (UltraTek Kit, ScyTek) in 0.05 mol/l Tris–HCl buffer at pH 7.6 containing 0.005% H_2O_2 for 10 min. The tissue sections were rinsed in distilled water, counterstained with hematoxylin, dehydrated with graded ethanol and xylene, and coverslipped. Different conditions were used for each primary antibody incubation. Primary antibody incubation was performed overnight with the following antibodies, shown in table 2 (**Tab. 1**): GAB1 (1:300 dilution, ab27439, Abcam), YAP 1 (1:200, sc101199, Santa Cruz Biotechnology), Filamin A (1:500 dilution, PM6/317, Fitzgerald Industries International), β-catenin (1:600 dilution, ab15180, Abcam BD Transduction Laboratories n° 610154), NPR3 (1:300 dilution, ab37617, Abcam), KCNA1 (1:1000, ab32433, Abcam), OTX2 (1:100, 1H12C4B5, Thermo Fisher), ATRX (1:1000 dilution, NBP1-83077 Novus Biologicals, rabbit polyclonal) and DAXX (1:150 dilution, HPA008736 Sigma rabbit polyclonal). Protein expression was quantified by counting stained tumor cells and/or nuclei over 1,000 cells in tumor regions considered as the most immunoreactive to determine the labeling index (LI). Cases with ≤15% of stained tumor cell nuclei were considered suggestive to harbour an ATRX mutation. Cytoplasmic-only reactivity and granular nuclear reactivity were considered as negative. β-catenin was scored as positive when ≥15% of neoplastic nuclei where stained, with either negative or positive cytoplasm (Fattet et al., 2009). GAB1, YAP1 and Filamin A were scored as positive when ≥20% of neoplastic cells showed staining intensity >1, while OTX2 and KCNA1 was scored as positive when ≥30% of cells showed staining

intensity ≥1,5; NPR3 when ≥40% of cells showed staining intensity ≥2.

ANTIGEN	ANTIBODY	DILUTION	POSITIVITY
GAB 1	ab27439, Abcam	1:200	≥20% cells with staining intensity >1+
YAP 1	sc101199, Santa Cruz Biotechnology	1:300	≥20% cells with staining intensity >1+
Filamin A	PM6/317, Fitzgerald Industries International	1:500	≥20% cells with staining intensity >1+
β-catenin	ab15180, Abcam BD Transduction Laboratories n° 610154	1:600	≥15% neoplastic nuclei with staining intensity ≥1+
NPR3	ab37617, Abcam	1:300	≥40% cells with staining intensity ≥2+
KCNA1	ab32433, Abcam	1:1000	≥30% cells with staining intensity ≥1,5+
OTX2	1H12C4B5, Thermo Fisher	1:100	≥30% nuclei with staining intensity ≥1,5+
ATRX	NBP1-83077 Novus Biologicals, rabbit polyclonal	1:1000	≤15% stained neoplastic nuclei were considered to harbour mutations
DAXX	HPA008736 Sigma rabbit polyclonal	1:150	Uncertain IHC results

Tab. 1: Antibodies used for IHC Analysis.

DNA extraction, PCR and sequencing analysis for hot spot mutations of H3.3, TERT promoter and CTNNB1

DNA from FFPE tumors was purified using the QIAamp DNA Mini Tissue Kit (Qiagen GmbH, Dusseldorf, Germany) according to the manufacturer's instructions after proteinase K digestion. Hematoxylin-Eosin (H&E) stained sections of each case were reviewed carefully by two independent neuropathologists before they were selected for DNA extraction. All samples selected contained at least 70% of vital tumor. Primers were designed to amplify the region containing TERT C228T and C250T hotspots, corresponding to the positions 124 and 146 Bp, respectively, upstream of the TERT ATG site. For H3.3 mutational analysis, primers contain the two mutations corresponding to LYS27 and GLY34. PCR conditions were for all the following: 95°Cx15 min, 94°Cx30 sec, 60°Cx30 sec (40 cycles), 72°CX30 sec, 72°CX10 min and 4°C. 5ul PCR fragments were then loaded on a 2% agarose gel and analyzed by Pyrosequencing. For Pyrosequencing analysis, single-stranded DNA templates were immobilized on streptavidin-coated Sepharose high-performance beads (GE Health

care, Uppsala, Sweden) using the PSQ Vacuum Prep Tool and Vacuum Prep Worktable (Biotage, Uppsala, Sweden), according to manufacturer's instructions, then incubated at 80°C for 2 minutes and allowed to anneal to 0.4 mmol/L sequencing primer at room temperature. Pyrosequencing was performed using PyroGold Reagents (Biotage) on the Pyromark Q24 instrument (Biotage), according to manufacturer's instructions. Controls in which the sequencing primer or template were omitted were used to detect background signal. Pyrograms were analyzed by using the Pyromark Q24 software (Biotage) using the allele quantification (AQ) software to determine the percentage of mutant versus wild-type alleles according to percentage relative peak height. A mutational screening of H3F3A (hotspot codons 27 and 34) and TERT promoter (hotspots C228 and C250) were carried out as previously reported (Gessi et al., 2014; Gielen et al., 2013). Furthermore, Sanger direct sequencing method was performed for metastatic MDB cases on purified PCR-products, spanning the mutation cluster region in exon 3 of CTNNB1, encompassing sequences encoding amino acids 30 to 45. Primer sequences to specifically amplify β-catenin gene were designed to lead to amplimers that cover nucleotides 791-1070 in exon 3 of Genbank reference sequence X89579, giving a product of 288 bp (Legoix et al., 1999). Sequencing was performed using an automated sequencer ABI 3730 equipped with 48 capillaries (Applied Biosystems) on template with 10 pmol of each oligo-primers. All the primers were described in table 3 (**Tab. 2**).

H3.3-Pyro PCR	
Primer forw: 5' tgtttggtagttgcatatgg 3'	Primer rev: 5'Biotin- tacaagagagactttgtcc 3'
Primer pyro: 5' caaaagccgctcgca 3'	
TERT mut -Pyro PCR	
Primer forw: 5' cctgccccttcaccttccag 3'	Primer rev: 5' Biotin-aggacgcagcgctgcctgaa 3'
Primer pyro: 5' accccgccccgtcccgacccc 3'	
CTNNB1 mut-PCR	
Primer-forw: 5′ tggaaccagacagaaaagcg 3′	Primer rev: 5′ ggacagtatgcaatgactcga 3′

Tab. 2: Sequence of primers used for Pyrosequencing Analysis and PCR analysis for Sanger sequencing.

DNA extraction, bisulfite modification and methylation-specific PCR (MS-PCR) for analysis of TERT promoter methylation status

The cohort analysed for UTSS methylation status consisted of 37 metastatic MDB and 25 pHGG. A quasi-quantitative methylation specific polymerase chain reaction was used to determine methylation status relative at the five CpG island-rich regions. DNA samples were prepared using the QIAamp DNA Mini Tissue Kit (Qiagen GmbH, Dusseldorf, Germany) according to the manufacturer's instructions. DNA was quantitated by Nanodrop 2000 Spectrophotometer (Thermo Electron North America LLC, West Palm Beach, FL). Bisulfite-modification of DNA samples for methylation analysis was conducted using the EZ DNA Methylation Kit from ZYMO Research (Irvine, CA). The five CpG island-rich promoter regions, –600 bp upstream of the transcription start site (UTSS region), were targeted using specific primers to amplify bisulfite modified DNA. A total of 2 pairs of primers were used, each pair comprised of a forward and a reverse primer specific for un-methylated and methylated alleles (**Tab. 3**). The primers targeting the un-methylated and methylated alleles yield 95 bp and 90 bp PCR products, respectively. Please also refer to human genome Refseq NC_000005.10 for detailed sequence information.

UTSS MS-PCR for methylated DNA	
Primer-forw: 5′ cgtgcggcgatttttggtcgt 3′	Primer-rev: 5′ cgtaatacccgaaacccgacgc 3′
UTSS MS-PCR for un-methylated DNA	
Primer-forw: 5’ aggtgtgtgtggtgatttttggttgt 3’	Primer-rev: 5’ cataatacccaaaacccaacaccccac 3’

Tab. 3: Sequence of primers used for Methylation-specific PCR (MS-PCR) analysis, specific for un-methylated and methylated alleles.

To determine linearity of amplification to make the MS-PCR quasi-quantitative, we first serially diluted tumor DNA samples (100 ng, 50 ng, 25 ng, 10 ng, 5 ng, 2 ng). Each diluted DNA sample was PCR amplified using primers targeting the un-methylated and methylated alleles at CpG island-rich region. The DNA concentration that falls within the linear phase of PCR amplification as visualized on the agarose gel was determined and used for subsequent PCR amplifications and quantitation of the samples.

In each reaction, we used also normal brain tissue as negative control and 2 positive controls: one DNA fully methylated and one DNA completely un-methylated, supplied by Chemicon. PCR reagents including Hot Start Platinum Taq DNA Polymerase (Invitrogen) and PCRs were performed on an ABI GeneAmp 9700 thermocycler. PCR conditions consisted of initial denaturing at 95 °C for 3 minutes; 38 cycles of 94 °C for 30 seconds, 58 °C for 30 seconds, 72 °C for 45 seconds, and final extension at 72 °C for 7 minutes. The PCR products were run in 2% agarose gels and visualized under ultraviolet lights with appropriate intensities to avoid saturation. The gel images were photographed using transilluminator and imaging system (Hartland, WI) and the acquired gel images were analyzed and digitalized using ImageJ Software. We used the primarily generated digitalized data for the comparative analysis between methylated alleles and un-methylated alleles. The Mean Intensity of the bands was measured using ImageJ Software and the intensity of the bands for methylated DNA were compared to intensity for un-methylated DNA for each sample to assign a specific Methylation Value (MV). UTSS region was considered hyper-methylated when the MV was ≥30% of the un-methylated DNA.

FSTL5 and ATRX gene expression analysis via RT-PCR

Formalin-fixed paraffin embedded tissue samples from 33 MDB and 27 pHGG patients containing more than 70% tumor cells, as evaluated by a pathologist from hematoxylin-eosin staining of sections, were included for gene expression analysis. Total RNA was extracted from tumor tissue sections using RNeasy FFPE Kit (Qiagen). For each sample, 0,25 μg of total RNA were reverse-transcribed using Superscript III (Invitrogen) with oligo(dT) priming according to the manufacturer's protocols. cDNA was then used as template in a 25 μl PCR reaction. Forward and reverse primers, shown in table 5 (**Tab. 4**), were designed on the bases of sequences deposited on NCBI for FSTL5 (Reference Sequence: NM_020116.4) and ATRX (Reference Sequence: NG_008838.1). To amplify the housekeeping gene HPRT1, used as internal reference control, was used the QuantiTect Primer Assay HPRT1 (Qiagen QT0059066), giving a product of 130 Bp. Each biomarker was amplified in parallel and simultaneously to the housekeeping gene for each patient sample analyzed. PCR cycling conditions were 95°C for 5', 35 cycles: 30" at 95°C, 30'' at 56-58°C, and 45" at 72°C; final extension 7'

at 72°C; finally, PCR products were visualized on a 2,5% agarose gel. The Mean Intensity of the bands for FSTL5 (133 bp) and ATRX (171 bp) was measured using ImageJ Software and compared with the intensity of the housekeeping band (HPRT1) for each sample to assign a specific Expression Value (EV). FSTL5, expressed at moderate levels in healthy brain tissue, was considered over-expressed when the EV was more than 110% of the EV housekeeping gene, down-expressed when the score was less than 90% of the EV housekeeping gene and normo-expressed when the score was between 110% - 90%. ATRX gene expression analysis was conducted in some cases to confirm results obtained via IHC.

ATRX RT-PCR	
Primer-forw: 5′ ccttgcacactcatcagaagaatc 3′	Primer-rev: 5′ cgtgacgatcctgaagacttgg 3′
FSTL5 RT-PCR	
Primer-forw: 5’ atgcagacggcataccaaag 3’	Primer-rev: 5’ tcttcatagcgcacatagct 3’

Tab. 4: Sequence of primers used for cDNA Semi-Quantitative Reverse Transcriptase-PCR analysis.

Fluorescence in situ Hybridization (FISH) for MYC and MYCN

Five-micron sections were cut from FFPE samples for FISH analysis of metastatic MDB. Slides were de-paraffinized in oven at 60°C for 60 min and incubated in xylene for 10 min. Slides were then dehydrated in ethanol and treated with pretreatment solution (1 mol/L sodium thiocyanate) for 30 min at 80°C; samples were immersed in pepsin solution (0,65% in protease buffer) for 20-30 min at 37°C, washed twice in buffer, and air-dried. The MYC or MYCN amplification was detected using LSI CMYC/CEP8 probe and LSI MYCN/CEP2 probe Vysis, in accordance with the manufacturer instructions (Abbott Laboratories). Sections were finally counterstained with DAPI, coverslipped, and stored in the dark at -20°C prior to analysis. FISH sections were examined with an Axio Imager M1 microscope (Carl Zeiss) equipped with Z-stack, using a 100x oil immersion objective, and analyzed by two investigators. Signals were counted in 100 tumor nuclei for each sample; an LSI/CEP signal ratio

between 1 and 2 was considered as gain. A signal ratio > 2 was considered as amplification.

Telomere-specific fluorescence in situ hybridization (Telo-FISH) and analysis using TeloView System

The presence of a canonical mechanism or alternative mechanism of telomere elongation has been investigated on consecutive sections, analyzing telomere length via FISH with FITC-PNA (Peptide Nucleic Acid) probes (Dako, K532511) complementary to the telomeric repeated sequences. The PNA probe does not recognize sub-telomeric sequences, allowing an exact measurement of the telomere length. Staining has been compared with endothelial cell nuclei as normal internal control.

Five μm sections were cut from FFPE tissues for FISH analysis. Slides were deparaffinized in an oven at 60°C for 60 min and incubated in xylene. Slides were then dehydrated in 100% ethanol for 5 min at room temperature (RT) and treated for 20 min at RT in 0.2 mol/L HCl, then with pre-treatment solution (1 mol/L sodium thiocyanate) for 30 min at 80°C. Slides were then incubated with 1 mg/mL pepsin in 0.01 mol/L HCl for 20 min at 37°C. The sample DNA was denatured at 80°C for 5 minutes together with fluorescein conjugated PNA probe. The hybridization was at 37°C for 2 hours, followed by a brief wash with a stringent solution at 65°C for 5 minutes. Cover slips were mounted with 2 x 10 μL antifade reagent containing DAPI as counterstain. FISH sections were examined with an AxioImager M1 microscope (Carl Zeiss Jena, Germany), using a 100x oil immersion objective and analyzed by two investigators. Signals were counted for at least 100 tumor cells; deconvolved images were converted into TIFF files and exported for telomere specific image analysis using the TeloView software program.

TeloView was a quantitative program that measures telomeres intensity within the nuclear space. Nuclear telomere analysis using TeloView determined the telomere numbers, telomere signal intensities and nuclear telomere distribution for each case. Quantitative telomere analysis was performed on ≥100 nuclei for patient. The integrated intensity of each telomere is calculated because it is proportional to the telomere length. A mean intensity of telomeres was measured for each case by TeloView, comparing

each telomere signal intensity with numbers of telomeres. We used positive and negative control cases for lengthening of telomeres to establish a threshold.

TeloView indicated the presence of two different telomeric profiles that are shown in figure 4 (**Fig. 6**), displaying significant differences in telomere length (p value<0,001) and number of telomeric aggregates for positive controls (brain tumors previously analysed with canonical or ALT activation) and negative controls (non-neoplastic brain tissues).

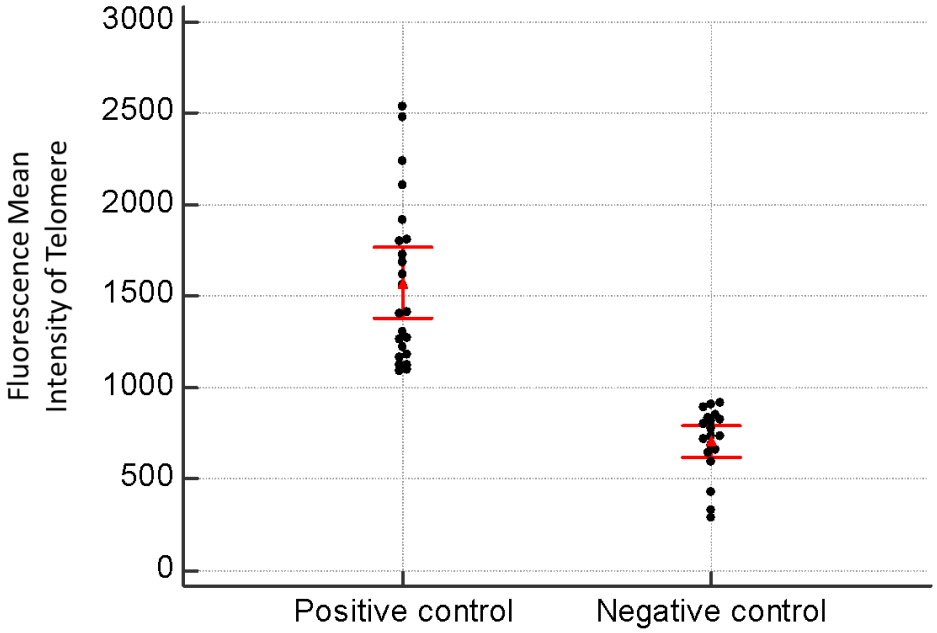

Fig. 6: Quantitative telomere analysis of positive and negative control cases using software TeloView. Spots evidenced the mean fluorescent intensity of each case.

Statistical analysis for overall survival and progression free survival

The association between categorical variables was tested using the Chi-square test. Overall survival (OS) and progression-free survival (PFS) were estimated using Kaplan–Meier method calculated from time of surgery. Overall survival was determined from the date of diagnosis to the date of death or last follow-up visit before death. PFS time was the interval from the date of starting chemotherapy to the date of progression or death, whichever occurred first, with censoring at the latest follow-up visit for alive and progression-free patients. The log-rank test was used to compare survival

information according to the prognostic factors. The multivariate Cox proportional hazards regression model was used to test the effect of prognostic factors on OS and PFS.

RESULTS

Molecular classification of metastatic medulloblastomas

Molecular subgrouping

According to the consensus molecular classification and biomarkers reported for MDB, we enrolled our samples in one of the four molecular subgroups, except 3 cases for which it was not possible to perform the analysis. We identified 5 WNT (14%), 7 SHH (19%), 9 group 3 (25%) and 6 group 4 (17%) cases; 9 MDB (25%) analyzed were not classified (N.C.) because did not share a define molecular profile with any of the four molecular subgroups.

Cases with triple immuno-positivity for GAB1, YAP1 and Filamin A were attributed to the SHH group; this molecular subgroup showed also 28% of cases with MYC amplification. Nuclear translocation of β-catenin identified WNT cases; OTX2 immuno-positivity also characterized group WNT medulloblastomas. CTNNB1 Sanger Sequencing was performed to evaluate mutations on exon 3, to confirm the presence of specific mutations that are involved in nuclear translocation of β-catenin. Results showed that no case (0/5, 0%) with nuclear immuno-positivity for β-catenin harbored mutations on cluster region in exon 3 of CTNNB1 gene, indicating that other mechanisms could be involved in β-catenin nuclear translocation and activation of WNT pathway in pediatric metastatic MDB. Immuno-positivity for NPR3 and OTX2, immuno-negativity for YAP1 and Filamin A, and amplification of MYC gene identified group 3 cases; amplification of MYC characterized 75% of group 3 cases, a higher frequency compared to the other subgroups. Group 4 cases were identified by immuno-positivity for KCNA1 and OTX2, immuno-negativity for YAP1 and Filamin A, and low expression of NPR3, which discriminate group 4 cases from group 3. Amplification of MYCN gene characterized only one case in our series of metastatic MDB, classified in group 4; no case of group 4 showed MYC amplification. MYC amplification was detected in 32.5% of our cases, a higher frequency compared to MYCN amplification (3%), while simultaneous amplification of both MYC and MYCN was not shown in any

case of our cohort (**Fig. 8**). Summary of IHC results and distribution within molecular subgroups was shown in figure 7 (**Fig. 7**).

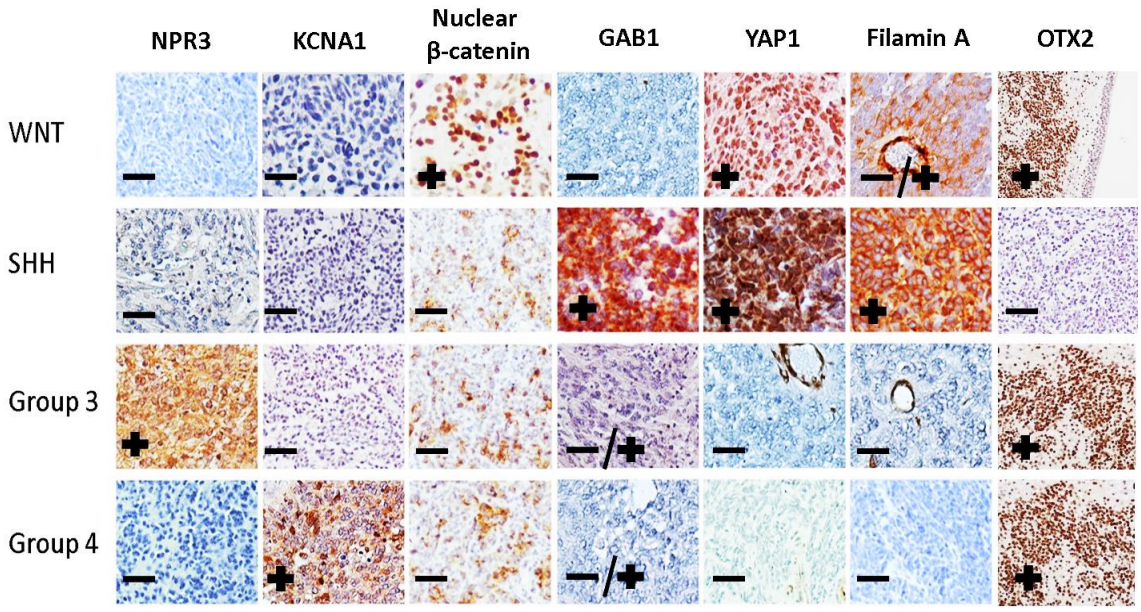

Fig. 7: Summary table of IHC presence/absence of proteins and distribution in molecular subgroups.

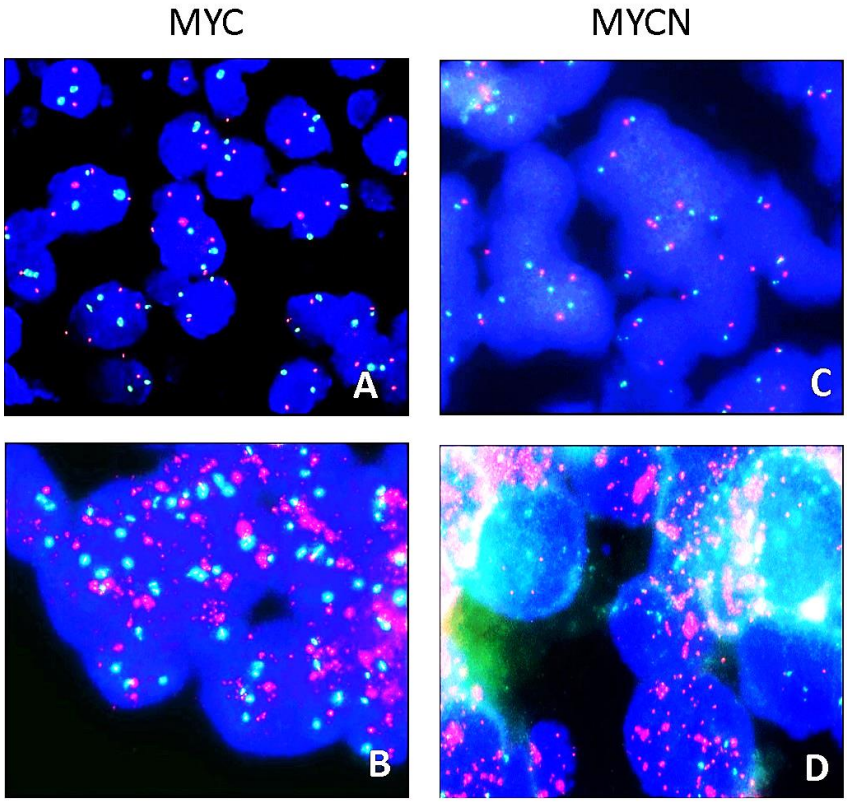

Fig. 8: Metastatic MDB selected cases with MYC not amplified (A), MYC amplification (B), MYCN not amplified (C) and MYCN amplification (D). MYC and MYCN probes were labelled with red fluorescent, CEP8 and CEP2 probes, using as internal references, were labelled in green.

Survival analysis of molecular subgroups

Kaplan–Meier curves of MDB subgroups obtained by molecular analysis were shown in figure 9 (**Fig. 9**). WNT and NC patients showed longer OS and PFS compared to the other molecular subgroups. The overall survival of group WNT and NC MDB was 100% in the first 70 months of treatment, furthermore no WNT or NC case relapsed in the first 40 months. The outcome of WNT and NC molecular subgroups of metastatic MDB was favorable, with a survival rate over 80% after a follow-up of 160 months. Conversely, SHH, group 3 and 4 medulloblastomas showed a similar trend in term of survival and were related to a worse outcome compared to WNT and NC, with a survival rate less than 60% after a follow-up of 160 months. The differences in terms of OS and PFS between WNT and NC MDB with group SHH, 3 and 4 cases were statistically significant (p value<0,05).

Finally, we also correlated the expression of each biomarkers with OS and PFS of patients (data not shown); none of the biomarkers analyzed showed significant association with outcome of metastatic cases.

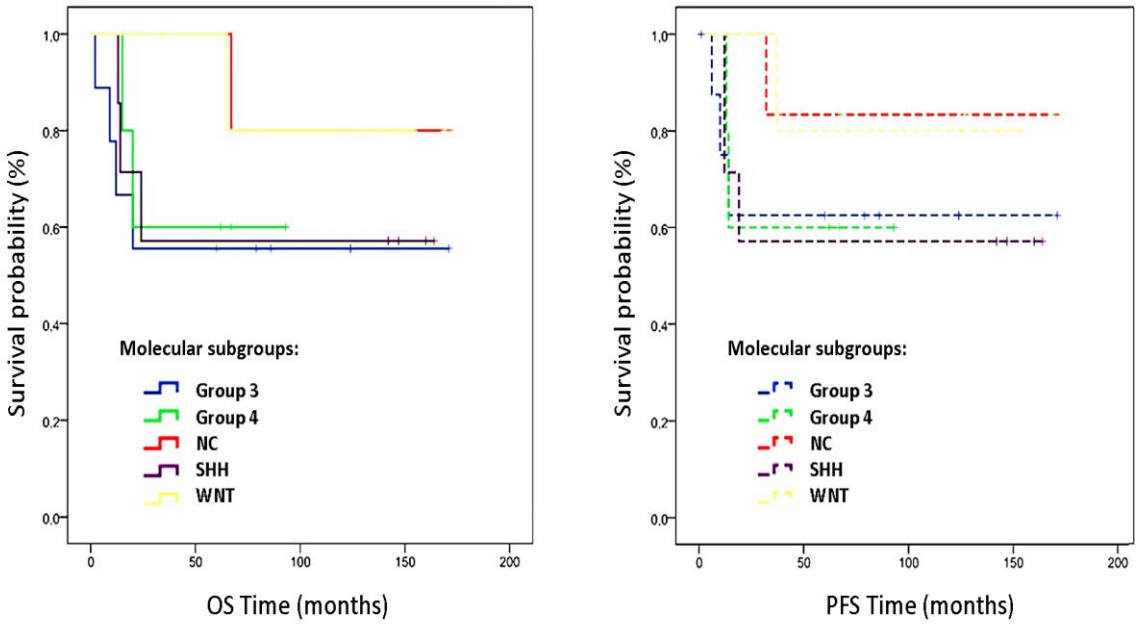

Fig. 9: Kaplan–Meier OS and PFS curves according to molecular subgroups: overall survival (solid line) and progression-free survival (dotted line). N.C. = not classified cases.

FSTL5

With the aim to investigate some molecular aspects involved in aggressiveness and invasion pathway in pediatric brain tumors, we analyzed the gene expression of FSTL5, a high-risk biomarker in primary MDB.

FSTL5 expression in metastatic MDB

Previous study revealed that FSTL5 play a role in MDB and was over-expressed in group C and high-risk group D tumors. FSTL5 over-expression was also significantly associated with reduced progression-free and overall survival across all disease variants in medulloblastomas not exclusively metastatic (Gilbertson et al., 2011; Northcott et al., 2011; Shih et al., 2014; Remke et al., 2011a). We evaluated FSTL5 expression levels and prognostic value in a series of MDB all with metastasis at the onset; FSTL5 expression analysis in our cases showed 9/33 (27%) metastatic MDB with over-expression, while 11/33 (34%) cases were characterized by down-expression; other cases showed FSTL5 normo-expression (13/33; 39%). Variation on FSLT5 expression levels among MDB cases was shown in figure 10 and 11 (**Fig. 10** and **Fig. 11**). The difference between FSTL5 down-expression, normo-expression and over-expression cases was statistically significant (p value<0,001).

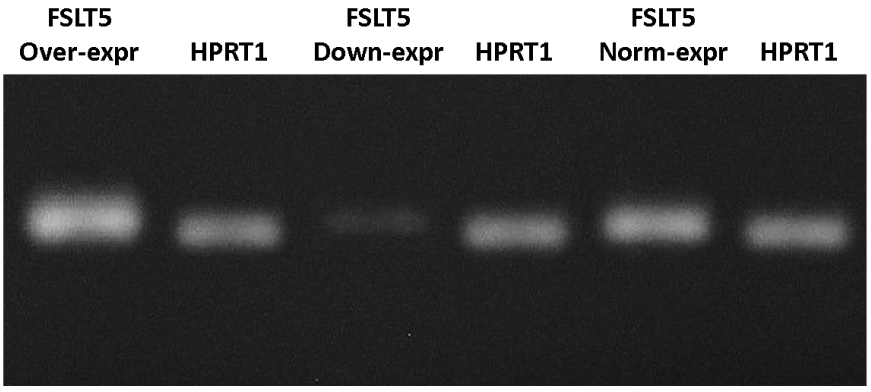

Fig. 10: A: Metastatic MDB selected cases with FSTL5 over-expression, down-expression and normo-expression compared to housekeeping gene HPRT1 in RT-PCR.

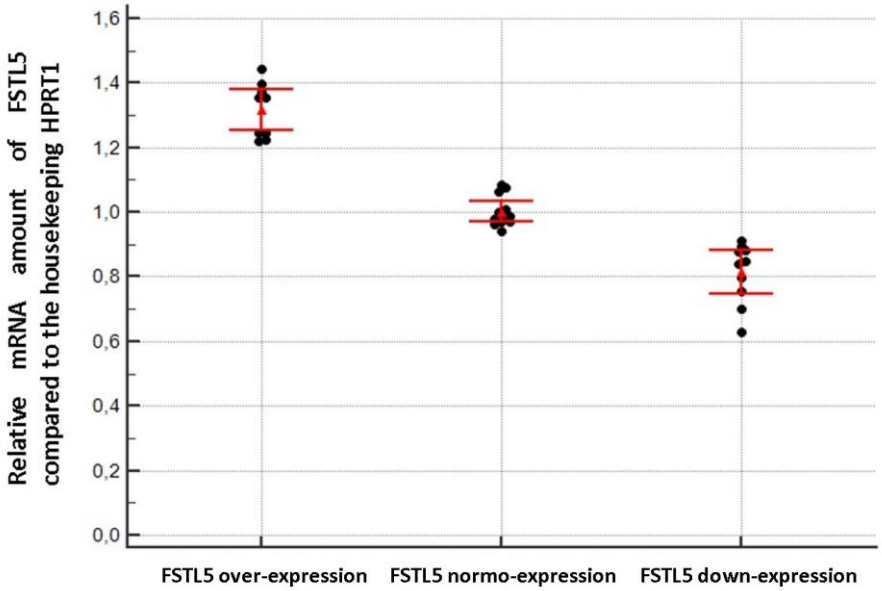

Fig. 11: Relative quantification of FSTL5 expression levels in metastatic MDB.

Group 3 and 4 metastatic MDB were characterized by higher expression levels of FSTL5 compared to WNT, SHH and NC subgroups (**Fig. 12**). The differences in expression levels of group 3/4 cases compared to the other subgroups were statistically significant (p value=0,006). FSTL5 expression analysis was performed also in 12 pediatric high-grade gliomas (pHHG), to compare results with those obtained for metastatic MDB. Medulloblastomas showed an over-expression in 27% of cases, while none of pHHG tested (0/12, 0%) for gene expression highlighted an over-expression, suggesting that FSTL5 is mostly expressed in brain tumors such medulloblastomas, and not in glia-derived tumor.

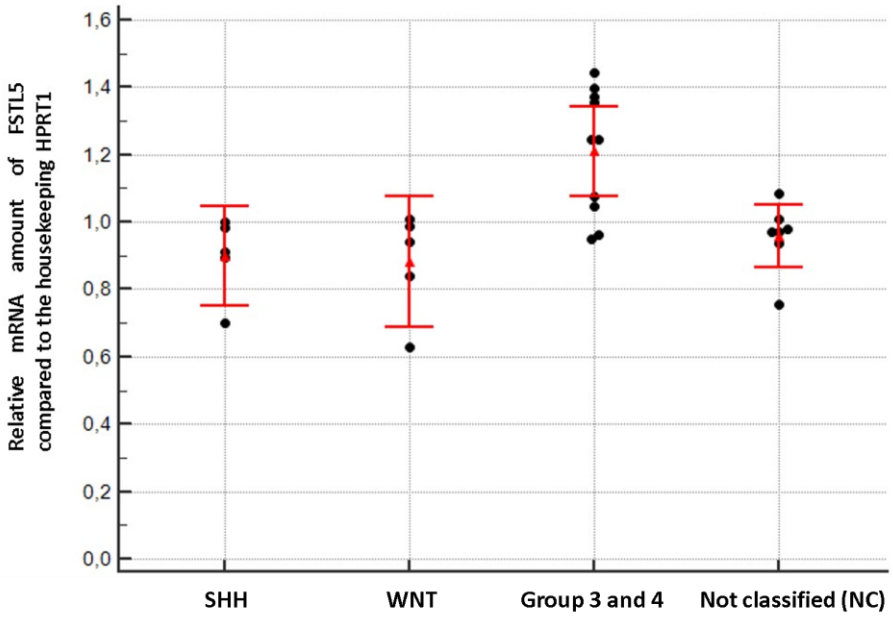

Fig. 12: Relative quantification of FSTL5 expression levels within different molecular subgroups.

Survival analysis and prognostic value of FSTL5 expression

Kaplan-Meier test revealed that metastatic MDB with high expression levels of FSTL5 correlated with worse prognosis compared to FSTL5 down-expression and normo-expression cases. Medulloblastomas with FSTL5 low-expression showed a survival rate around 90%, while cases with over-expression were characterized by a survival rate less than 50% after a follow-up of 160 months (**Fig. 13**); the differences, in terms of OS and PFS, were statistically significant (p value<0,05).

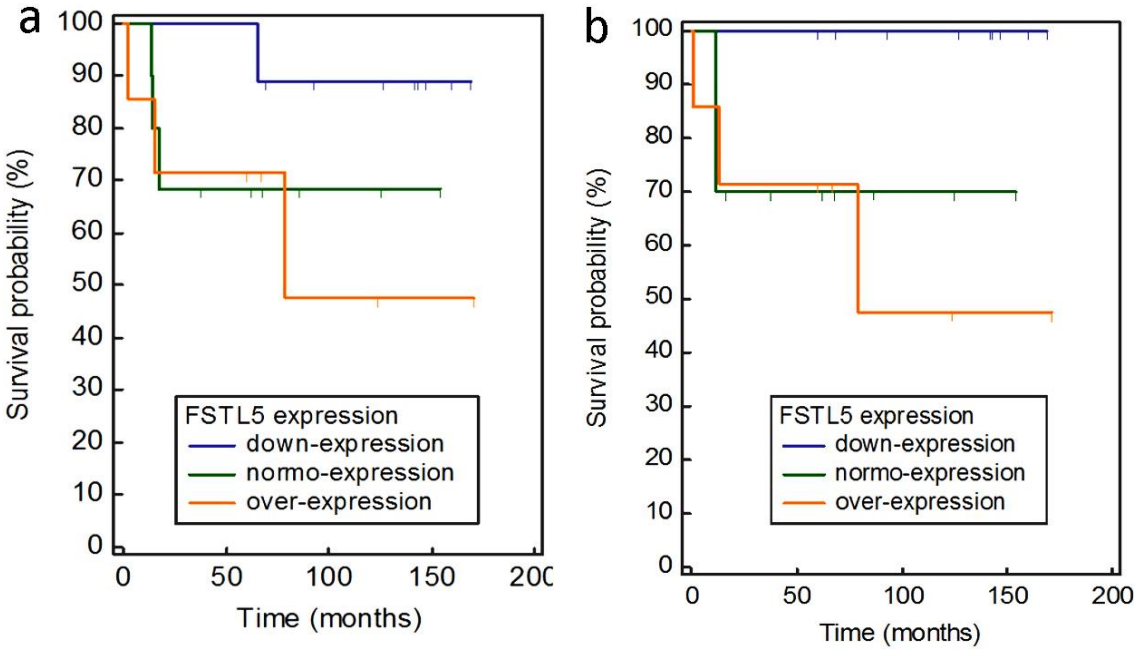

Fig. 13: Kaplan Meyer analysis of overall survival (a) and progression-free survival (b) according to FSTL5 expression levels in metastatic MDB.

FSTL5 molecular mechanism involved in tumor growth and cellular migration

FSTL5 is a biomarker for MDB, however, its biological functions and molecular mechanisms in cancer development are poorly understood. FSTL5 is a secretory protein with sub-cellular localization. The molecular function of FSTL5 was not so clear, but this gene includes calcium ion binding domain. Calcium-binding proteins participate in calcium cell signalling pathways by binding to Ca^{2+}, the calcium ion that plays an important role in many cellular processes. FSTL5 has calcium-ion-storage activity, interacting selectively with Ca^{2+} and might be involved in regulating tumor microenvironment; in fact, calcium signalling can be activated in cells with pathological conditions, leading to environment changing (Yang et al., 2010). Remodel of Ca^{2+} homeostasis affects cell cycle regulators, such p21 and Cdc25C, leading to tumor growth and angiogenesis; furthermore, high extracellular levels of Ca^{2+} promote Ras and Rac1 activity, Pyk2 phosphorylation and activation of others calcium ions dependent effectors involved in cell migration and invasion. Elevated extracellular Ca^{2+} can also activate calcium-sensing receptors (CaSR), that increase phosphorylation of ERK2 and Akt promoting b1-integrin cell surface expression and cellular migration (Tharmalingam et al., 2016).

We hypothesize a molecular mechanism, shown in figure 14 (**Fig. 14**), in which FSLT5 over-expression leads to increase secretion of this protein binding Ca^{2+}, that affects tumor microenvironment and sustains the most aggressive MDB cells associated with high risk subgroups.

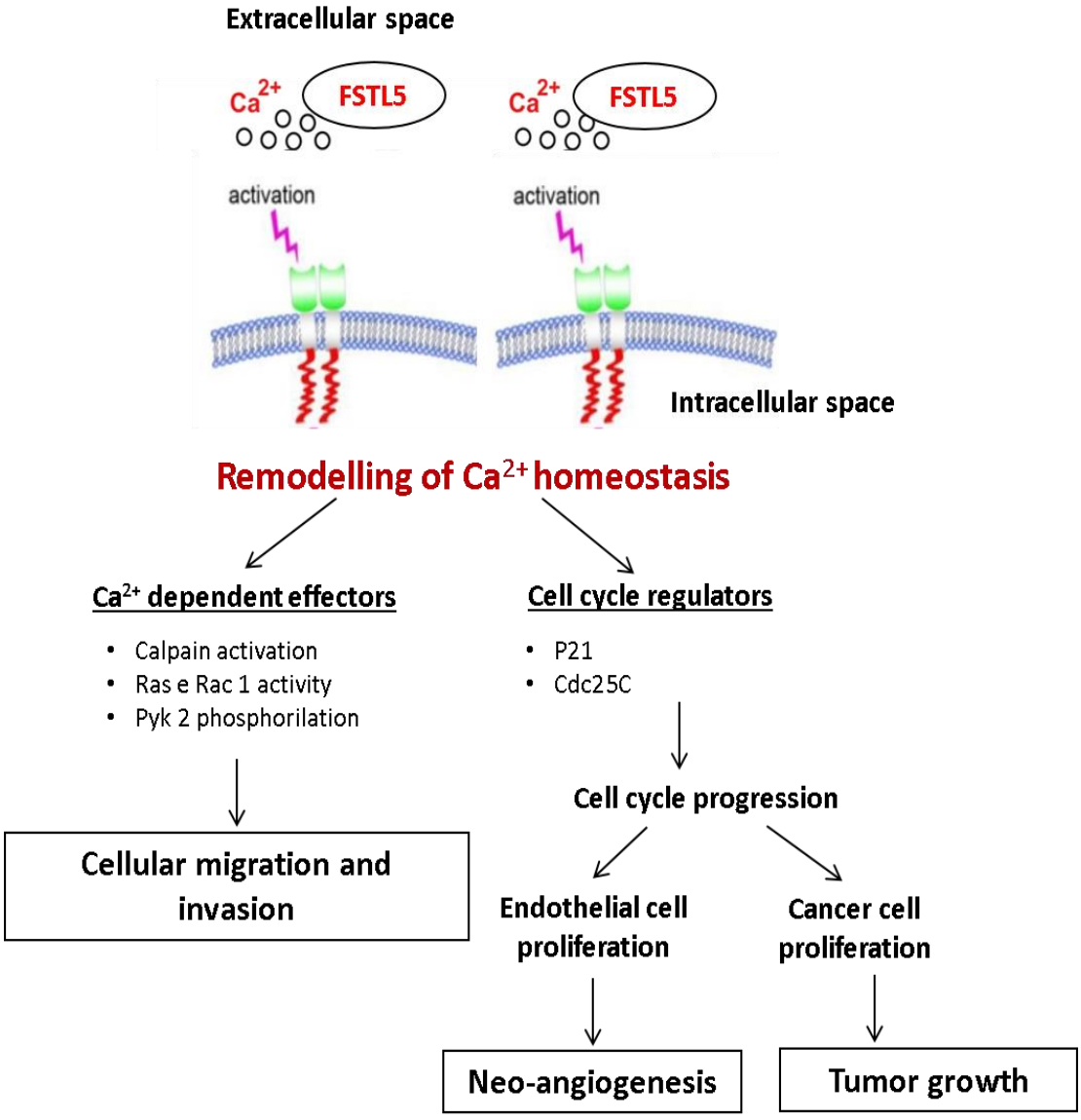

Fig. 14: Our hypothesis of FSTL5 molecular mechanism by binding Ca^{2+}, triggering the activation of several pathways involved in cellular migration, angiogenesis and proliferation.

Control of telomeres elongation in metastatic MDB and pHGG

Study of telomere lengthening control and pathways involved in senescence escape was conducted to evaluate molecular and genetic bases of these mechanisms in aggressive form of pediatric brain tumors. We screened a cohort of 39 pediatric metastatic MDB and a series of 55 pHGG for evidence of telomere length elongation, using telomere-specific FISH (Telo-FISH). Since the presence of mutations in ATRX results in loss of nuclear expression, we assessed the nuclear staining via IHC (**Fig. 15**). H3.3 and TERT promoter hot spot mutations were analyzed by pyrosequencing (**Fig. 16** and **Fig. 17**, respectively), while epigenetic status of UTSS region was analyzed by methylation-specific-PCR (**Fig. 18**). Regarding DAXX protein expression analysis, the lack of reproducibility of the IHC technique for DAXX immunostaining made dubious and uncertain our results, both for metastatic MDB and pHGG. Results obtained for DAXX were not considered for telomere lengthening activation (data not shown).

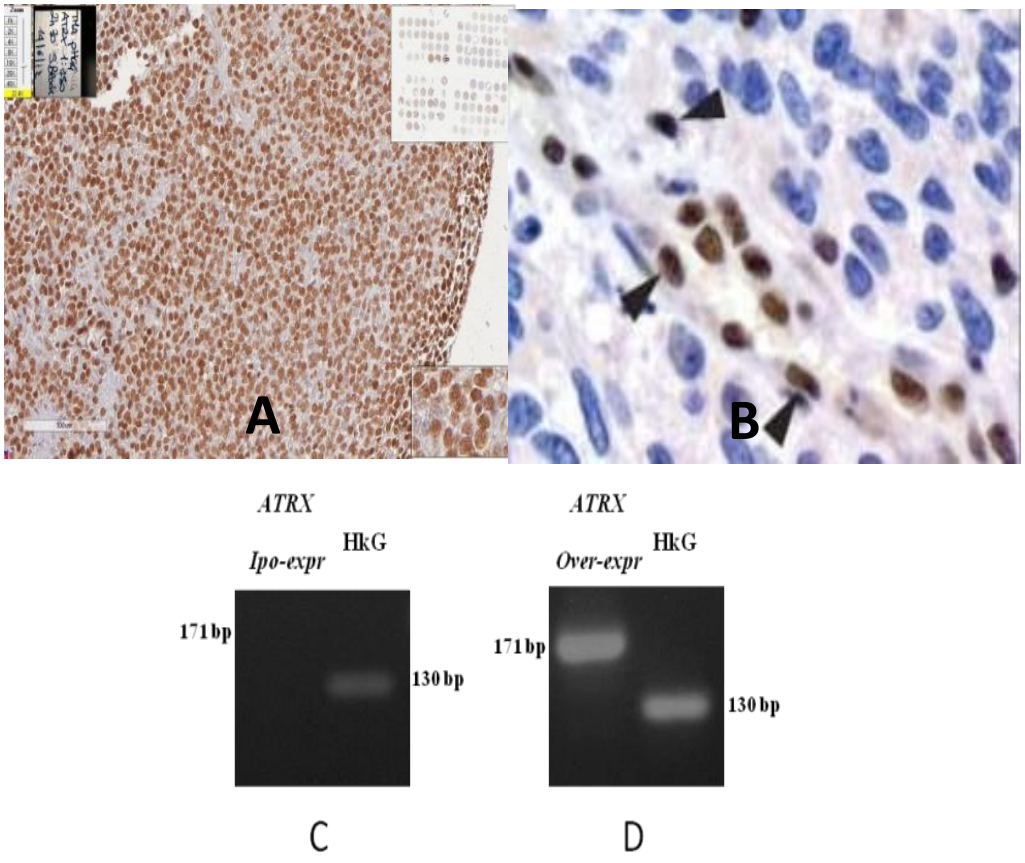

Fig. 15: A) 100% nuclear immunopositivity for ATRX in a selected case on TMA. B) Selected case with nuclear immunonegativity for ATRX (arrows indicate endothelial cells as internal positive control). C) Selected case with ATRX down-expressed in RT-PCR. D) Selected case with ATRX over-expression in RT-PCR. (HkG: *HPRT1 housekeeping gene).*

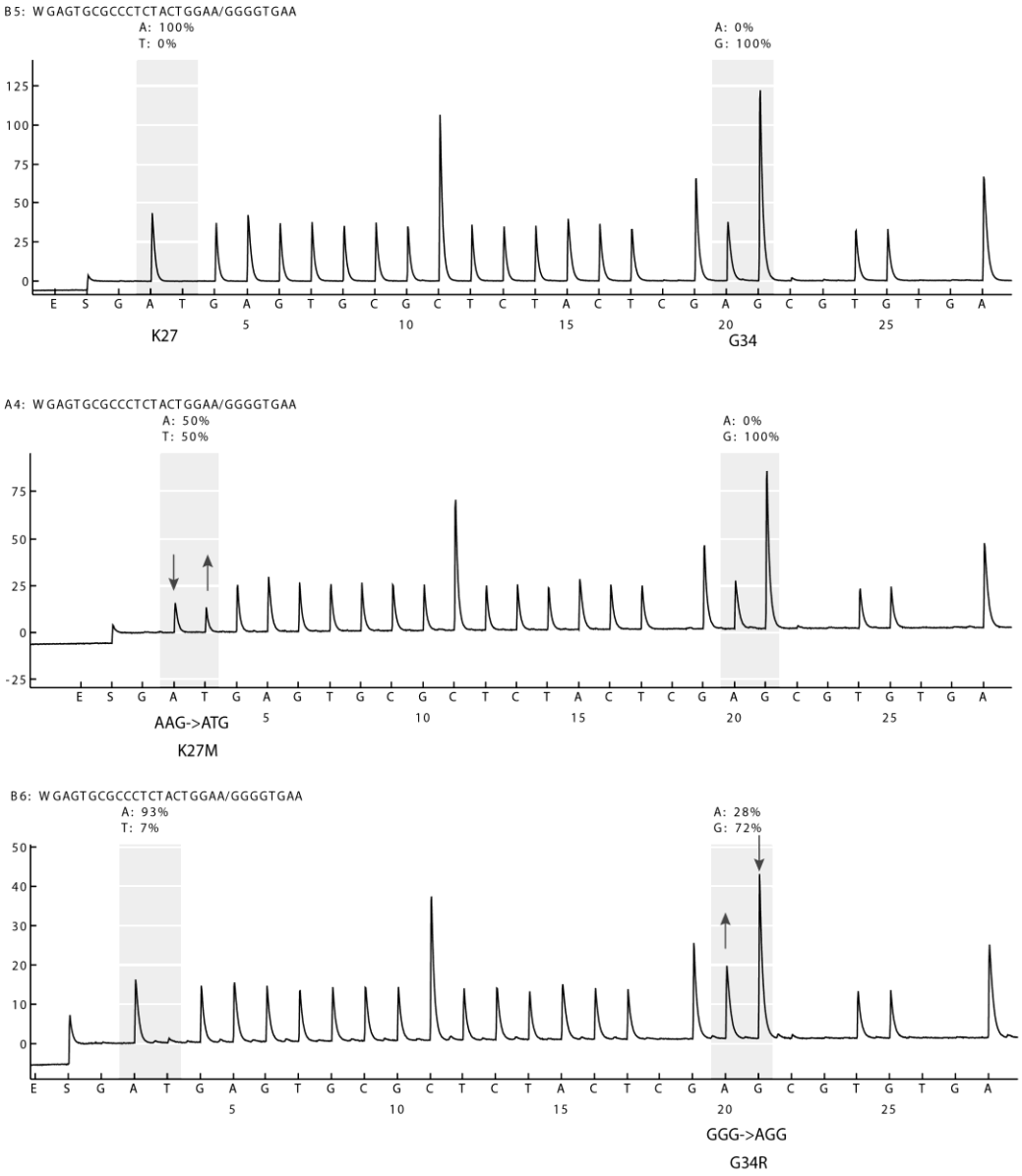

Fig. 16: From the top: Selected WT case, Selected case with H3.3 K27M mutation and selected case with H3.3 G34R mutation.

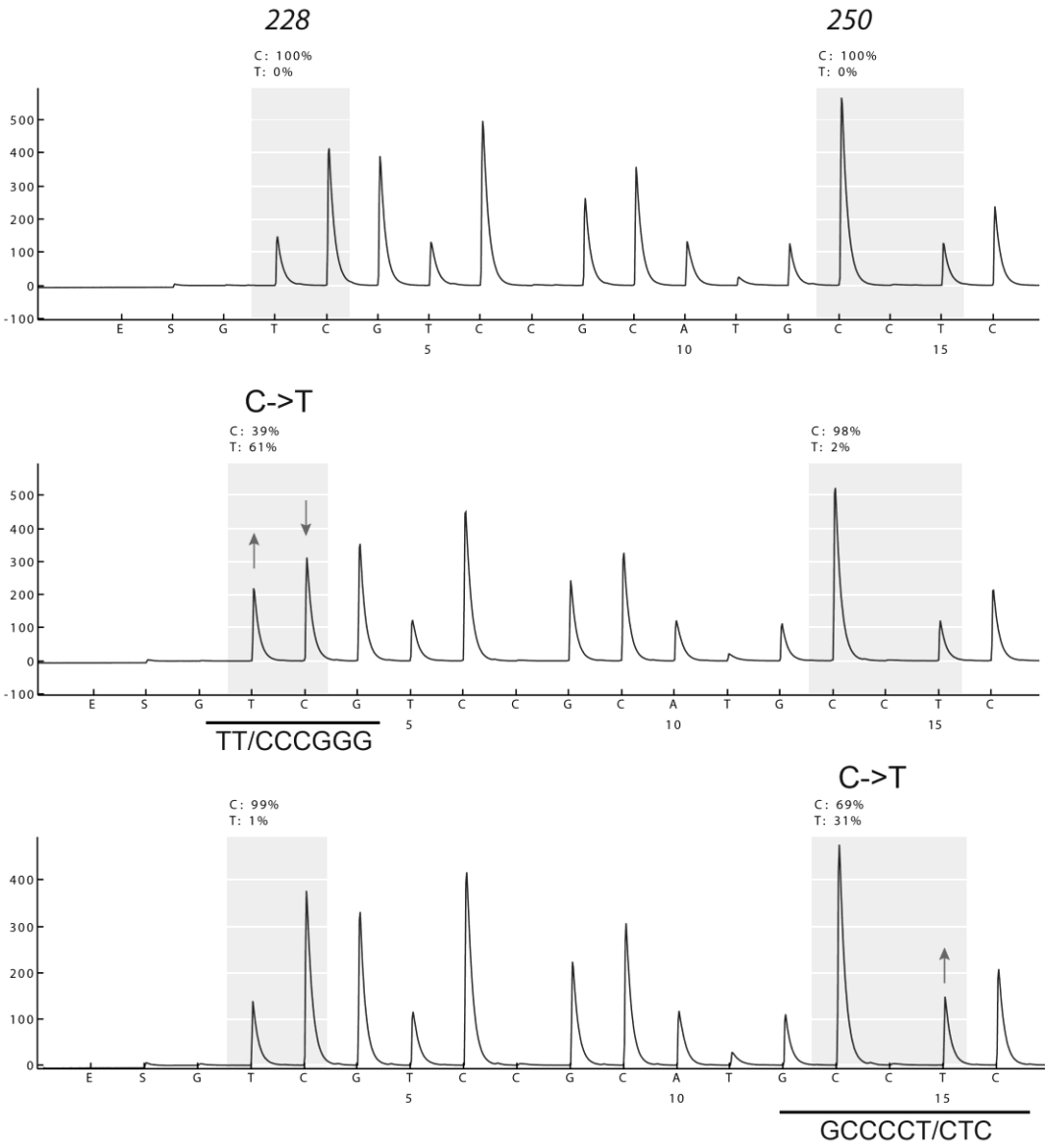

Fig. 17: From the top: Selected WT case, Selected case with TERT C228T mutation and selected case with TERT C250T mutation.

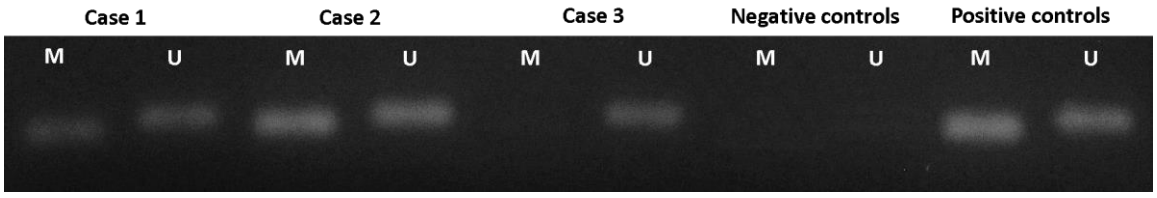

Fig. 18: Selected cases with UTSS hyper-methylated (Case 1 and 2) and not methylated (Case 3) in MS-PCR; positive and negative controls were included in each experiment.

Genetic and molecular alterations of factors involved in pathways of telomere length control

Among metastatic MDB, none of these cases showed H3.3 mutations (0/20, 0%), while 6 cases (6/29; 20,6%) showed TERT mutations: 5 cases with TERT C250T mutation and 1 with TERT C228T mutation. ATRX nuclear loss characterized 28% (7/25) metastatic medulloblastomas. Study of TERT promoter methylation status in UTSS region showed that 22 metastatic MDB (22/37, 59,5%) were characterized by hyper-methylation, with a methylation value ≥30%. Pediatric high-grade gliomas showed the presence of H3.3 mutations in 9 cases (9/42, 21,4%): 6 cases with LYS27 mutation and 3 with GLY34 mutation. TERT mutations characterized only 2 cases (2/26, 7,6%) of pHGG analyzed, all with C250T mutation; loss of ATRX nuclear expression was evidenced in 11 pHGG (11/52, 21%), that did not show nuclear staining. We used a RT-PCR analysis approach for confirming some samples (n=7) in which the IHC staining for ATRX was unclear; gene expression confirmed IHC results in analyzed cases. Furthermore, 7 pHGG (7/25, 28%) were hyper-methylated in UTSS region of TERT.

These findings underlined that hyper-methylation in UTSS region was more frequent in metastatic MDB, as well as TERT promoter mutation, compared to pHGG. Conversely, H3.3 mutations did not characterize metastatic medulloblastomas but only pHGG; ATRX nuclear loss was shown both in metastatic MDB and pHGG, with similar incidence. Notably, ATRX loss and TERT mutations were mutually exclusive, except for one medulloblastoma case. Within molecular subgroups of metastatic medulloblastomas, alterations in different factors involved in control of telomere elongation were found in all molecular subgroups, with less frequencies in subgroup four, regarding TERT promoter mutations and UTSS hyper-methylation. Within pHGG, the percentage of cases with ATRX, H3.3, TERT and UTSS alterations differed according to the histopathological type of tumors. H3.3 mutations, TERT promoter mutations and ATRX nuclear loss were detected in most cases of GBM and AA, in contrast to other histologies which include 6 pilocytic astrocytomas, 5 ganglioneuronal and 4 primitive neuroectodermic tumors, and 1 oligoastrocytoma. Furthermore, UTSS hyper-methylation characterized GBM with high incidence, in contrast to anaplastic astrocytomas and other histologies, in which only a small percentage of the tumors harbored this alteration.

Elongation of telomeres

Metastatic MDB and pHGG cases with alterations in telomeres lengthening control pathways were tested via Telo-FISH to evaluate the elongation of telomeres (**Fig. 19**); cases with no alterations in ATRX, H3.3 or TERT were also analyzed.

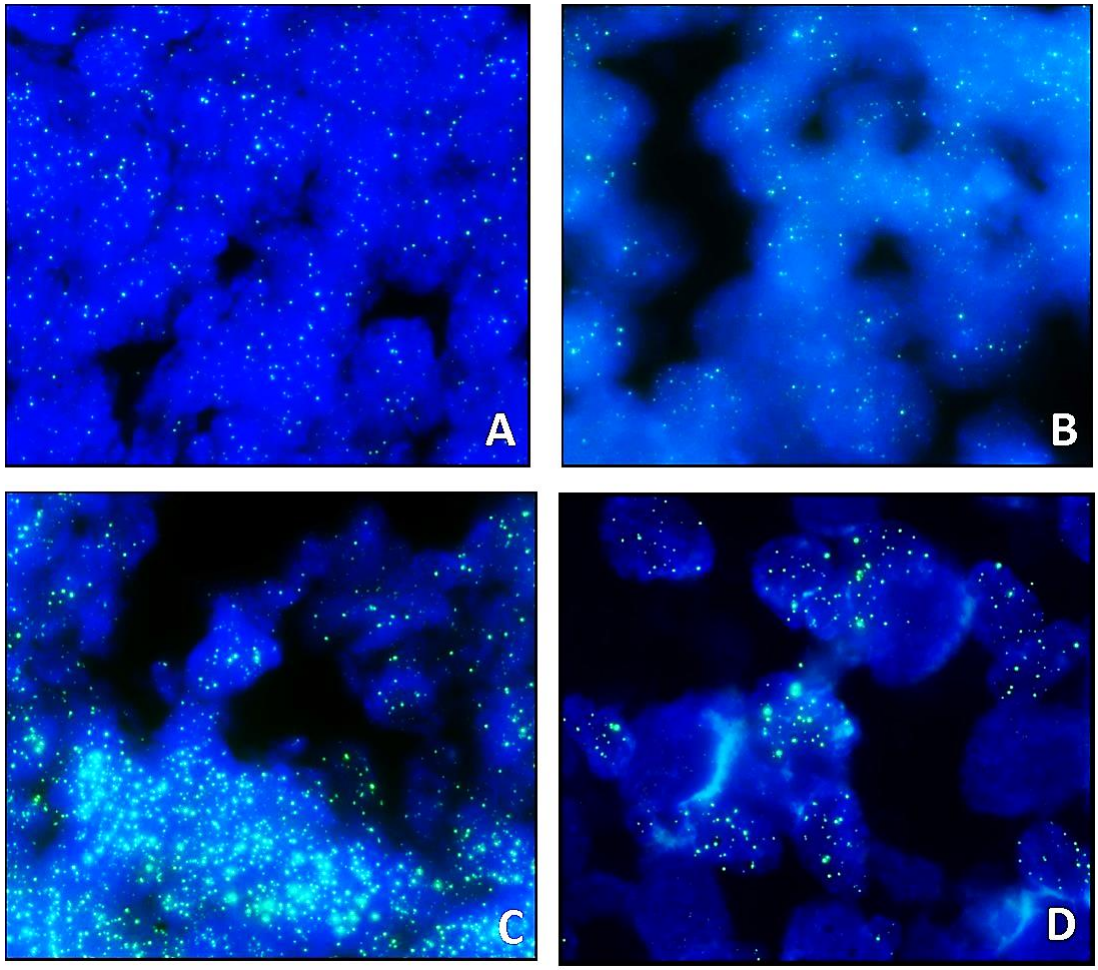

Fig. 19: Telo-FISH analysis of telomere length in metastatic MDB (A, C) and pHGG (B, D). Green signals evidenced telomeric sequences. Representative images of telomere-specific fluorescence in situ hybridization show elongation of telomere length in metastatic MDB (C) and pHGG (D) versus tumor cells with basal levels of telomere length in medulloblastomas (A) and high-grade gliomas (B).

Metastatic MDB showed 9 cases (9/22, 41%) with elongation of telomeres; pHGG were characterized by 40% of cases (12/30) with increase of telomere length. All other cases showed basal levels of telomere length, with significantly reduced intensity of fluorescence signals. These findings underlined that elongation of telomeres characterize both metastatic medulloblastomas and pediatric high grade gliomas with

similar incidence. Within molecular subgroups of MDB, cases with telomere length increasing were found in all molecular subgroups, with less frequency in subgroup 4; while, among pHGG, telomere elongation was detected with high incidence in GBM and AA, in contrast to other histologies in which no case (0%) showed increase of telomere length.

Results of ATRX nuclear loss, H3.3 and TERT promoter mutations, UTSS hyper-methylation and elongation of telomeres in metastatic MDB and pHGG, stratified by molecular subgroups and histological diagnosis, were shown in table 5 (**Tab. 5**).

Tumor type	n° of cases	H-TERT mutations (%)	H3.3 mutations (%)	ATRX nuclear loss (%)	UTSS hypermethylation (%)	Telomere elongation (%)
Metastatic MDB	**39 cases**	**20,6% (6/29)**	**0% (0/20)**	**28% (7/25)**	**59,5% (22/37)**	**41% (9/22)**
SHH	7 cases	20% (1/5)	0% (0/4)	20% (1/5)	71,4% (5/7)	40% (2/5)
WNT	5 cases	40% (2/4)	0% (0/3)	25% (1/4)	75% (3/4)	50% (2/4)
Group 3	9 cases	16,6% (1/6)	0% (0/3)	33,3% (2/6)	66,6% (6/9)	50% (2/4)
Group 4	6 cases	0% (0/5)	0% (0/3)	25% (1/4)	16,6% (1/6)	25% (1/4)
Not classified (NC)	12 cases	22,2% (2/9)	0% (0/7)	33,3% (2/6)	63,6% (7/11)	40% (2/5)
pHGG	**55 cases**	**7,6% (2/26)**	**21,4% (9/42)**	**21% (11/52)**	**28% (7/25)**	**40% (12/30)**
GBM	28 cases	7,6% (1/13)	18% (4/22)	30,7% (8/26)	37,5% (6/16)	53,3% (8/15)
AA	11 cases	20% (1/5)	55,5% (5/9)	18% (2/11)	0% (0/3)	50% (4/8)
Others histologies	16 cases	0% (0/8)	0% (0/11)	6,6% (1/15)	16,6% (1/6)	0% (0/7)

Tab. 5: Summary of results for ATRX, H3.3, TERT, UTSS and telomere elongation, with frequency of alterations within metastatic MDB and pHGG.

Canonical elongation of telomeres, ALT detection and association with ATRX, H3.3, TERT and UTSS alterations

We used a software program (TeloView) that measures telomere intensity signals within the nuclear space to determine telomeres elongation in our cases. Positive and negative control cases were used to establish a threshold and to identify different telomeric profiles, indicative of cases with increase of telomere length or not.

Twenty-two metastatic medulloblastomas were analysed and the mean intensity of telomeres for each case was measured. Results (**Fig. 20**) showed that cases with ATRX nuclear loss were always associated with telomere elongation (6/6, 100%), with a significantly increased fluorescence signals, comparable to intensities of the positive controls and indicative of ALT activation.

Medulloblastomas with TERT promoter mutations were correlated with increase telomere length (4/5, 80%), but only in cases with UTSS hyper-methylated. Canonical pathway of telomere elongation via telomerase reactivation was shown in metastatic MDB with TERT promoter mutations in combination with hyper-methylation of UTSS; telomere elongation was not present when TERT promoter was mutated but UTSS region was un-methylated. Telomere elongation was not found in cases without alterations of TERT or ATRX (0/12, 0%); all these wild type cases showed a significantly reduced fluorescence signals and the mean intensities of telomeres were comparable to those of the negative controls. Furthermore, UTSS hyper-methylation in metastatic MDB was not sufficient alone to activate elongation of telomeres.

The differences in telomere length of cases with ATRX alterations compared to wild type medulloblastomas were statistically significant (p value=0,0019).

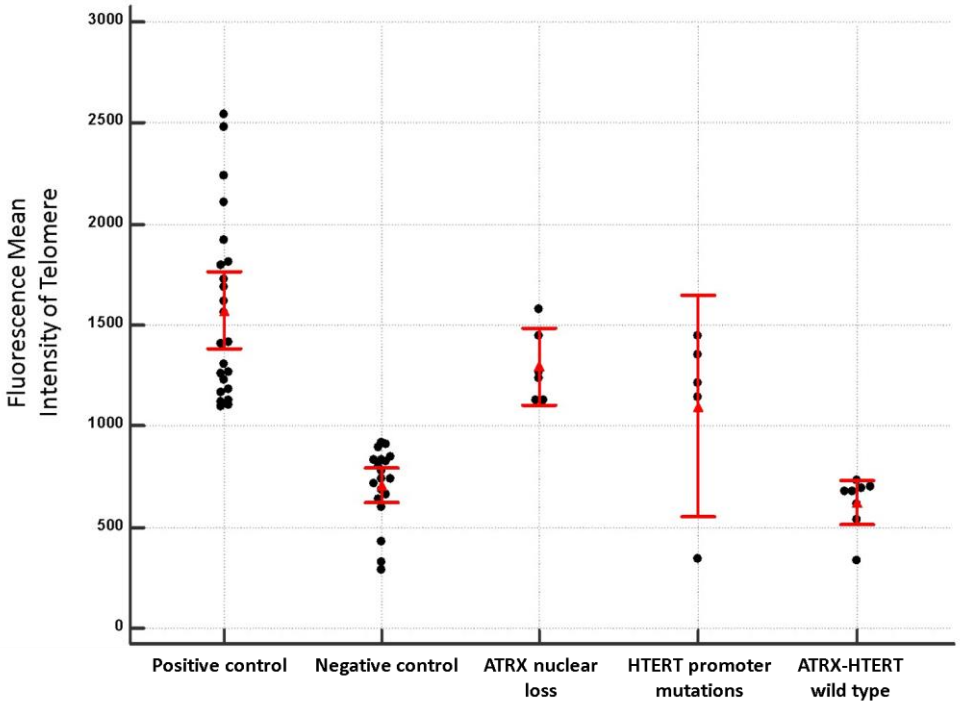

Fig. 20: Quantification of fluorescence intensity of telomeres for metastatic medulloblastomas within different groups characterized by ATRX nuclear loss, TERT promoter mutations or no alterations. Analysis of telomere length for positive and negative control cases were included.

Thirty pediatric high-grade gliomas were also analysed to measure the mean intensity of telomeres for each case. Results (**Fig. 21**) showed that telomere elongation was present in all cases with ATRX nuclear loss (9/9, 100%). Elongation was found also in cases with positive nuclear staining for ATRX, in presence of H3.3 GLY34 or H3.3 LYS27 mutations. All cases with mutated H3.3 GLY34 were correlated with increase telomere length (3/3, 100%), while only 2 patients with H3.3 LYS27 mutation were associated with elongation of telomeres (2/6, 33,3%). These findings highlighted that mutations in GLY34 of histone H3.3 and/or ATRX nuclear loss always activated ALT and increased telomere length of pHGG. Telomere elongation was not present when TERT promoter was mutated (0/2, 0%); furthermore, telomere length increase was not shown in cases with no alterations of TERT, H3.3 or ATRX (0/12, 0%). Wild type and TERT mutated cases showed a significantly reduced fluorescence signals, with the mean intensities of telomeres comparable to those of the negative controls. In pHGG, as well as in metastatic MDB, UTSS hyper-methylation alone did not activate elongation of telomeres.

The differences in telomere length of cases with ATRX and/or H3.3 alterations, compared to TERT mutated and wild type gliomas, were statistically significant (p value=0,0066).

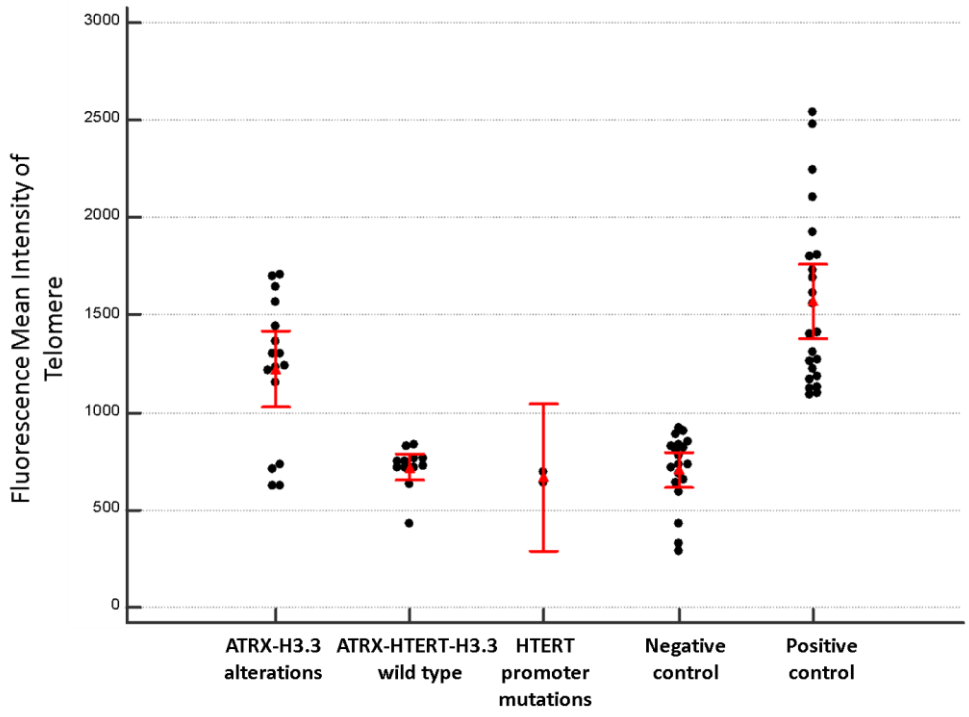

Fig. 21: Quantification of fluorescence intensity of telomeres for pediatric high-grade gliomas within different groups characterized by ATRX nuclear loss and/or H3.3 mutations, TERT promoter mutations or no alterations. Analysis of telomere length for positive and negative control cases were included.

Our results highlighted that metastatic medulloblastomas could control elongation of telomeres via canonical pathway of telomerase reactivation (3/22, 13,6%), induced by TERT promoter mutations in combination with UTSS hyper-methylation, or ALT mechanism (6/22, 27,3%), induced by ATRX alteration; while, our pediatric high-grade gliomas increased telomere length only via the alternative pathway ALT (12/30, 40%), induced by ATRX or H3.3 alterations.

DISCUSSION

This research was conducted to investigate a large cohort of medulloblastomas with leptomeningeal dissemination at the onset. Nowadays, research in the field of pediatric neuro-oncology is focused on biomolecular characterization of pediatric tumors to treat these cancers more adequately.

Various studies indicated molecular subgrouping correlation with age distribution, biological behavior and prognostic stratification of MDB (Ellison et al., 2011a; Ellison et al., 2011b; Ellison et al., 2005; Kool et al., 2008; Korshunov et al., 2012; Northcott et al., 2011; Northcott at al., 2012a; Ramaswamy et al., 2016; Remke et al., 2011a and b; Robinson et al., 2012; Taylor et al., 2012). These studies included only a small percentage of metastatic cases at the onset; in fact, the percentage of metastatic cases did not exceed 30% and were not studied independently from the non-metastatic counterpart.

In this work, we analyzed a series of 39 pediatric metastatic MDB according to the molecular classification consensus (Ellison et al., 2011a; Ellison et al., 2011b; Northcott at al., 2012b; Ramaswamy et al., 2016; Taylor et al., 2012). In order to classify our metastatic cases according to molecular subgroups, we evaluated protein expression of GAB1, YAP1, Filamin A, β-catenin, NPR3, OTX2 and KCNA1, gene expression levels of FSTL5 and amplification of MYC and MYCN gene, with a sub-classification system widely available.

We identified 14% WNT, 19% SHH, 25% group 3 and 17% group 4 cases, while 25% of MDB analyzed were not classified (N.C.) on the basis of these biomarkers; molecular classification highlighted the presence of metastatic medulloblastomas in WNT subgroup, characterized by nuclear translocation of β-catenin (Fattet et al., 2009) and absence of FSTL5 over-expression. CTNNB1 Sanger Sequencing, performed to evaluate mutations on exon 3 in cases with nuclear translocation of β-catenin, showed that 0/5 (0%) cases with nuclear immuno-positivity for β-catenin harbored mutations on cluster region in exon 3 of the gene. Despite the absence of mutations, WNT cases highlighted a good prognosis, indicating that also other mechanisms could be involved in β-catenin nuclear translocation and could influenced outcome of patients.

Evaluation of nuclear translocation of β-catenin by IHC in metastatic MDB allowed a good sub-classification of patients and risk stratification of cases.

Various studies showed molecular subgrouping correlation with outcome of pediatric patients, but some survival information remain unknown for metastatic MDB (Ramaswamy et al., 2016). Recently, the relevance of subgroup status and biologic parameters (WNT/MYCC/MYCN status) in a homogeneous prospective trial population of 121 metastatic MDB was confirmed (Van Bueren et al., 2016), showing the prognostic role of WNT activation in metastatic disease. Four patients with metastatic WNT-activated medulloblastoma survived without relapse, indicating that WNT-metastatic MDB may be treated successfully by less intensive treatment regimens (standard risk protocol) (Van Bueren et al., 2016).

Biomarkers analysis allowed us to identify five WNT metastatic cases in our cohort, associated with good outcome with a survival rate >80% after a follow-up of 160 months. Molecular classification was useful to identify WNT metastatic medulloblastomas and define outcome of these cases, considered standard risk patients as recently proposed in literature (Van Bueren et al., 2016). Not classified medulloblastomas, a subgroup of metastatic MDB that did not share a define molecular profile with any of the four molecular subgroups, were related also to good prognosis, similar to WNT group.

In literature, group 3 cases with metastasis at the onset have been identified as being very high risk, while metastatic cases of group SHH and group 4 were considered high risk patients (Ramaswamy et al., 2013; Ramaswamy et al., 2016; Shih et al., 2014; Van Bueren et al., 2016). Our results confirmed this risk stratification of patients with metastatic spread at diagnosis; in fact, our survival curves for SHH, group 3 and 4 cases, obtained with molecular classification, showed all an association with bad outcome and survival rate <60% after a follow-up of 160 months.

FSTL5 over-expression in MDB, with other factors of malignancy such MYC/MYCN amplification, was associated with high risk subgroups and correlated with poor prognosis (Gilbertson et al., 2011; Northcott et al., 2011; Remke et al., 2011a). This work confirmed that FSTL5 expression can be used as an excellent marker for discrimination of metastatic MDB in different molecular subgroups: group 3 and group 4, characterized by FSTL5 high expression levels, and group SHH/WNT/NC, characterized by FSTL5 low expression levels. Furthermore, survival curves showed an association between over-expression of FSTL5 and bad outcome of patients,

characterized by a survival rate <50%, while medulloblastomas with FSTL5 down-expression highlighted a survival rate of 90%.

We showed that FSTL5 is an independent prognostic marker for metastatic MDB; furthermore, none of pHHG tested for FSTL5 gene expression highlighted an over-expression, suggesting that FSTL5 is mostly over-expressed in medulloblastomas and not in glia-derived tumor.

FSTL5 is a second effector of cell survival, proliferation and migration; it's a secret glycoprotein which regulates activin and other TGFβ family members. We hypothesized that FSTL5 interacts with Ca^{2+} in extra-cellular space and regulates tumor microenvironment. Calcium, as extra-cellular messenger, is essential signal transduction element (Yang et al., 2010) and the dysregulation of Ca^{2+} homeostasis is an important event in driving the expression of the malignant phenotypes, such as proliferation, migration, invasion, and metastasis (Yih-Fung Chen et al., 2013; Tharmalingam et al., 2016).

In conclusion, calcium dysregulation induced by FSTL5 over-expression can trigger to migration, invasiveness and malignancy in high-risk subgroups of metastatic MDB. The addition of FSTL5 expression analysis to existing molecular stratification schemes can be considered a reliable tool for prognostic evaluation in clinical trials of medulloblastomas with metastatic spread at diagnosis.

In the light of the knowledge on the cell survival and senescence escape, we also investigated molecular mechanisms to maintain telomere length in pediatric brain tumors, especially in medulloblastomas with leptomeningeal dissemination at the onset; in fact, our goal was to analyze the possible activation of mechanisms involved in control of telomere lengthening, via telomerase reactivation or ALT.

Elongation of telomeres is necessary for tumor cell immortalization and senescence escape; this could be obtained by a reactivation of telomerase or by a telomerase-independent pathway called ALT (Ceccarelli et al., 2016; Cesare et al., 2010; Koelsche et al., 2013; Mangerel et al., 2014; Remke, Ramaswamy et al., 2013). ALT mechanism is due to alterations in H3.3 or ATRX genes, reported in pediatric gliomas and correlated with increase of telomere length (Heapy, de Wilde et al., 2011; Heapy, Subhawong et al., 2011; Schwartzentruber J et al., 2012).

We screened a cohort of 39 pediatric metastatic MDB and 56 pHGG to evaluate the length of telomeres, ATRX nuclear loss, H3.3 and TERT promoter mutations and UTSS methylation status. The understanding of molecular mechanisms to maintain telomere

length in PBT, especially in metastatic medulloblastomas, can improve knowledge about tumour cells escape from replicative senescence.

Previous studied revealed that ALT was highly activated in high-grade gliomas, but rarely found in medulloblastomas (Dorris et al., 2014; Mangerel et al., 2014). We observed ALT in our cohort of pediatric high grade gliomas (40%), associated with H3.3 and ATRX alterations. ALT was not found only in pHGG, but it was a mechanism activated also in pediatric metastatic medulloblastomas with high incidence (27,3%). ALT pathway is activated with higher frequency in our metastatic cases compared to non-metastatic medulloblastomas analysed in literature (<5%) (Dorris et al., 2014; Mangerel et al., 2014). The observation that ALT is highly activated in MDB with metastasis highlights the biological differences between metastatic and non-metastatic medulloblastomas in control of telomere elongation, cells immortalization and senescence escape.

As reported in literature (Ceccarelli et al., 2016; Ebrahimi et al., 2016; Gielen et al., 2013; Heapy, de Wilde et al., 2011), telomeres length elongation was strongly correlated with ATRX nuclear loss in our work, showing a significantly increased intensity of fluorescence signals indicative of ALT. H3.3 mutations, considered a driving oncogenetic event in a significant subgroup of pHGG (Sturm et al., 2012), did not affect our medulloblastomas (0%), suggesting that telomere elongation by ALT is only activated via ATRX alterations in metastatic MDB. As previously analyzed in literature (Gielen et al., 2013; Heapy, de Wilde et al., 2011; Schwartzentruber J et al., 2012), we observed H3.3 mutations in pHGG; however, these mutations were not always associated with elongation of telomeres. Results highlighted that mutations in GLY34 of histone H3.3 were always correlated with increase telomere length (100%), while H3.3 LYS37 mutations activated ALT with less incidence (33,3%).

Most cancers maintain their telomere length through reactivation of telomerase and not ALT, triggered by specific mutations in the TERT promoter; however, this is uncommon in pediatric cancer (Killela et al., 2013; Koelsche et al., 2013). As reported in previous studies (Killela et al., 2013; Koelsche et al., 2013; Nonoguchi et al., 2013), TERT promoter mutations were rare in our cohort of pHGG (7,6%), while pediatric metastatic medulloblastomas harboured these alterations more frequently (20,6%). Previous work conducted on primary medulloblastomas reported a high frequency of TERT mutation in SHH subgroup (Remke, Ramaswamy et al., 2013). Conversely, we found that all molecular subgroups of metastatic medulloblastomas were characterized

by alterations in ALT-activating factors or telomerase, with less frequency for subgroup 4.

Furthermore, a specific region of TERT promoter called UTSS was found to be hyper-methylated in high grade brain tumors and not hyper-methylated in normal tissues and low-grade tumours in literature (Castelo-Branco et al., 2013). Our results underlined that hyper-methylation in UTSS region was more frequent in metastatic MDB (59,5%) compared to pHGG (28%), as well as TERT promoter mutation. Within our gliomas cohort, UTSS hyper-methylation characterized GBM with high incidence (37,5%), in contrast to astrocytomas and other histologies, in which only a small percentage of tumors harbored this alteration. Our results support the finding that UTSS hyper-methylation is associated with tumour progression and aggressive histological variants of pediatric brain tumors.

Previous study suggested that hyper-methylation of UTSS cause also over-expression of TERT to maintain telomere length in PBT (Castelo-Branco et al., 2013). We showed that hyper-methylation in UTSS region was not sufficient alone to activate elongation of telomeres. We also evidenced that TERT promoter mutations were not always associated with elongation of telomeres; TERT promoter mutations correlated with increase of telomeres length only in association with UTSS hyper-methylation in our medulloblastomas. This observation suggested that TERT promoter mutations and UTSS hyper-methylation act together, increasing TERT expression and telomeres length via telomerase reactivation for metastatic MDB (13,6%).

In conclusion, we found cases with elongation of telomeres in our cohorts of metastatic medulloblastomas (41%,) and pediatric high grade gliomas (40%). We highlighted that medulloblastomas with metastasis at the onset could control elongation of telomeres both via canonical pathway of telomerase reactivation, induced by TERT promoter mutations in combination with UTSS hyper-methylation, or ALT mechanism, induced only by ATRX alterations and not H3.3 mutations. There was almost mutual exclusivity between ALT and TERT promoter mutations for all analysed cases. Results for pediatric high grade gliomas suggested that pHGG did not elongate telomeres via telomerase reactivation (0%), but exclusively via the alternative pathway ALT, induced by ATRX and/or H3.3 alterations. Therefore, pediatric metastatic medulloblastomas seem to have a major activation of the canonical pathway and different involvement in molecular control of telomeres elongation compared to pediatric gliomas.

Recent data showed that ALT activation could attenuate the poor outcome in some pediatric brain tumors (Ceccarelli et al., 2016; Dorris et al., 2014); analysis of telomere length maintenance via telomerase or ALT may contribute to risk stratification of patients and targeted therapies to improve outcome for these children. Further validation on a larger prospective cohort will determine the effect of ALT and telomerase reactivation on the outcome of pediatric high grade gliomas and metastatic medulloblastomas.

CONCLUSION

Our aim was to study specific molecular alterations involved in the processes of metastasis and cell survival in a series of 39 pediatric medulloblastomas with leptomeningeal dissemination at the onset. In fact, no gold standard treatment has been defined for metastatic MDB, and pediatric neuro-oncology research is focused on biomolecular characterization of these tumors, to treat patients with more appropriate therapies.

First of all, we evaluated the prognostic relevance of the four molecular subgroups, with a sub-classification system widely available, in order to define risk classes for patients with leptomeningeal dissemination at diagnosis.

Interestingly, the molecular features of medulloblastoma with metastasis at the onset are very similar compared to non-metastatic MDB. In fact, we showed that distribution of metastatic cases into four molecular subgroups, reflecting a high molecular heterogeneity, is highly similar to the frequency of non-metastatic ones.

This work highlighted that our molecular subgrouping system could allow a risk stratification of metastatic medulloblastomas, to define high-risk patients (group SHH, 3 and 4), with a survival rate <60%, and standard-risk patients (group WNT), with a survival rate >80%.

In the future, we will extend the study of metastatic cohort under investigation to analyze the tumor cells genome methylation profiling, in order to classify samples that could not be attributed to any of subgroups basing on the markers so far analyzed.

We also evidenced that FSTL5 over-expression was associated with poor outcome of patients, with survival rate <50%; FSTL5 gene expression can be used to better define outcome of patients with metastasis at the onset and to stratify these cases in different risk classes. The addition of FSTL5 expression analysis to existing molecular stratification schemes can constitute a reliable and cost-effective tool for prognostic evaluation in future clinical trials of metastatic MDB.

Since FSTL5 is a glycoprotein which interacts with Ca^{2+} in extra-cellular space, we hypothesized that calcium dysregulation induced by FSTL5 over-expression can trigger to migration, invasiveness and malignancy of cells in high-risk subgroups of metastatic medulloblastomas.

Furthermore, we evaluated the possible activation of a pathway controlling elongation of telomeres, via the reactivation of telomerase or via ALT mechanism.

Interestingly, we evidenced that medulloblastomas with metastasis at the onset control elongation of telomeres both via canonical pathway of telomerase reactivation and via ALT mechanism. ALT pathway is activated with higher frequency (27,3%) in our metastatic cases compared to non-metastatic MDB analyzed in literature (<5%), and is strongly associated with ATRX nuclear loss, while H3.3 mutations do not affect metastatic MDB.

The observation that ALT is highly activated in our cohort highlights the biological differences between metastatic and non-metastatic medulloblastomas in control of telomere elongation, cells immortalization and senescence escape.

Metastatic MDB have a higher activation of the canonical pathway of telomerase reactivation (13,6%) compared to pHGG (0%), induced by TERT promoter mutations in combination with UTSS hyper-methylation. UTSS hyper-methylation characterized our metastatic MDB with high incidence (59,5%) and could be associated with malignancy and invasiveness of these cases.

Our findings suggest that immortalization of tumor cells in metastatic MDB is a common process to escape from the replicative senescence.

Analysis of telomere elongation in medulloblastomas and other pediatric high-grade brain tumors via telomerase reactivation or ALT may contribute to risk stratification of patients and future development of targeted therapies. Further studies will be necessary to allow better classification and risk stratification, in order to identify aggressive tumors, requiring more invasive therapy, and patients with favorable prognosis, who might benefit from a reduction of chemotherapy and radiotherapy dosage.

BIBLIOGRAPHY

1. Antonelli M, Buttarelli FR, Arcella A, Nobusawa S, Donofrio V, Oghaki H, Giangaspero F (2010). Prognostic significance of histological grading, p53 status, YKL-40 expression, and IDH1 mutations in pediatric high-grade gliomas. J Neurooncol 5:209–215.

2. Batra V, Sands SA, Holmes E, Russell Geyer J, Yates A, Becker L, Burger P, Gilles F, Wisoff F, Allen JC, Pollack IF, Finlay JL (2014). Long-term survival of children less than six years of age enrolled on the CCG-945 phase III trial for newly-diagnosed high-grade glioma: a report from the Children's Oncology Group. Pediatr Blood Cancer 61:151–157.

3. Bechter OE, Zou Y, Shay JW, Wright WE (2003). Homologous recombination in human telomerase-positive and ALT cells occurs with the same frequency. EMBO Rep 4:1138–1143.

4. Castelo-Branco P, Zhang C, Lipman T, Fujitani M, Hansford L, Clarke I, Harley CB, Tressler R, Malkin D, Walker E, Kaplan DR, Dirks P, Tabori U (2011). Neural tumor-initiating cells have distinct telomere maintenance and can be safely targeted for telomerase inhibition. Clin Cancer Res 17(1):111–121.

5. Castelo-Branco P, Sanaa C, Mack S, Gallagher D, Zhang C, Lipman T, Zhukova N, Walker EJ, Martin D, Merino D, Wasserman JD, Elizabeth C, Alon N, Zhang L, Hovestadt V, Kool M, Jones DTW, Zadeh G, Croul S, Hawkins C, Hitzler J, Wang JCY, Baruchel S, Dirks PB, Malkin D, Pfister S, Taylor MD, Weksberg R, Tabori U (2013). Methylation of the TERT promoter and risk stratification of childhood brain tumours: an integrative genomic and molecular study. Lancet Oncol 2013; 14: 534–42.

6. Ceccarelli M, Barthel FP, Malta TM, Sabedot TS, Salama SR, Murray BA, Morozova O, Newton Y, Radenbaugh A, Pagnotta SM, Anjum S, Wang J, Manyam G, Zoppoli P, Ling S, Rao AA, Grifford M, Cherniack AD, Zhang H, Poisson L, Carlotti Jr CG, Pretti D, Tirapelli DC, Rao A, Mikkelsen T, Lau CC, Yung WKA, Rabadan R, Huse J, Brat DJ, Lehman NL, Barnholtz-Sloan JS, Zheng S, Hess K, Rao G, Meyerson M, Beroukhim R, Cooper L, Akbani R, Wrensch M, Haussler D, Aldape KD, Laird PW, Gutmann DH, Iavarone A,Verhaak RGW (2016). Molecular Profiling Reveals Biologically Discrete Subsets and Pathways of Progression in Diffuse Glioma. Cell 164, 550–563 January 28, 2016. doi.org/10.1016/j.cell.2015.12.028.

7. Cesare AJ, Reddel RR (2010). Alternative lengthening of telomeres: models, mechanisms and implications. Nat Rev Genet 11:319–330.

8. Cifuentes-Rojas C, Shippen DE (2012) Telomerase regulation. Mutat Res 730:20–27.

9. De Braganca KC, Packer RJ (2013) Treatment options for medulloblastoma and CNS primitive neuroectodermal tumor (PNET). Curr Treat Options Neurol 15:593–606.

10. Dong Z, Siegel P, Kulozik AE, Zapatka M, Guha A, Malkin D, Felsberg J, Reifenberger G, von Deimling A, Ichimura K, Collins VP, Witt H, Milde T, Witt O, Zhang C, Castelo-Branco P, Lichter P, Faury D, Tabori U, Plass C, Majewski J, Pfister SM, Jabado N (2012). Driver mutations in histone H3.3 and chromatin remodelling genes in paediatric glioblastoma. Nature 482:226–231.

11. Dorris K, Sobo M, Onar-Thomas A, Panditharatna E, Stevenson CB, Gardner SL, DeWire MD, Pierson CR, Olshefski R, Rempel SA, Goldman S, Miles L. Fouladi M, Drissi R (2014). Prognostic Significance of Telomere Maintenance Mechanisms in Pediatric High-Grade Gliomas. J Neurooncol. 2014 March; 117(1): 67–76. doi:10.1007/s11060-014-1374-9.

12. Ebrahimi A, Skardelly M, Bonzheim I, Ott I, Mühleisen, Eckert F, Tabatabai G, Schittenhelm J (2106). ATRX immunostaining predicts IDH and H3F3A status in gliomas. Acta Neuropathologica Communications 4:60. doi 10.1186/s40478-016-0331-6.

13. Ellison DW (2010). Childhood medulloblastoma: novel approaches to the classification of a heterogeneous disease. Acta Neuropathologica, 120(3), 305–16. doi:10.1007/s00401-010-0726-6.

14. Ellison DW, Dalton J, Kocak M, Nicholson SL, Fraga C, Neale G, … Gilbertson RJ (2011a). Medulloblastoma: clinicopathological correlates of SHH, WNT, and non-SHH/WNT molecular subgroups. Acta Neuropathologica, 121(3), 381–96. doi:10.1007/s00401-011-0800-8.

15. Ellison, DW, Kocak M, Dalton J, Megahed H, Lusher ME, Ryan SL, … Clifford SC (2011b). Definition of disease-risk stratification groups in childhood medulloblastoma using combined clinical, pathologic, and molecular variables. Journal of Clinical Oncology : Official Journal of the American Society of Clinical Oncology, 29(11), 1400–7. doi:10.1200/JCO.2010.30.2810.

16. Ellison DW, Onilude OE, Lindsey JC, Lusher ME, Weston CL, Taylor RE, … Clifford SC (2005). beta-Catenin status predicts a favorable outcome in childhood medulloblastoma: the United Kingdom Children's Cancer Study Group Brain Tumour Committee. Journal of Clinical Oncology : Official Journal of the American Society of Clinical Oncology, 23(31), 7951–7. doi:10.1200/JCO.2005.01.5479.

17. Episkopou H, Draskovic I, Van Beneden A, Tilman G, Mattiussi M, Gobin M, Arnoult N, Londono-Vallejo A, Decottignies A (2014). Alternative lengthening of telomeres is characterized by reduced compaction of telomeric chromatin. Nucleic Acids Res 42:4391–4405.

18. Fattet, S, Haberler, C, Legoix, P, Varlet, P, & Lellouch-tubiana A (2009). Beta-catenin status in paediatric medulloblastomas : correlation of immunohistochemical expression with mutational status , genetic profiles , and clinical characteristics. Journal of Pathology, 86–94. doi:10.1002/path.

19. Gandola, L, Massimino, M., Cefalo G, Solero C, Spreafico F, Pecori E, Riva D, Collini P, Pignoli E, Giangaspero F, Luksch R, Berretta S, Poggi G, Biassoni V, Ferrari A, Pollo B, Favre C, Sardi I, Terenziani M, Fossati-Bellani F (2009). Hyperfractionated Accelerated Radiotherapy in the Milan Strategy for Metastatic Medulloblastoma. Journal of Clinical Oncology, Vol 27, No 4 pp. 566-571.

20. Gessi M, Van De Nes J, Griewank K, Barresi V, Buckland ME, Kirfel J, Caltabiano R, Hammes J, Lauriola L, Pietsch T, Waha A (2014). Absence of TERT promoter mutations in primary melanocytic tumors of the central nervous system. Neuropathol Appl Neurobiol 40(6):794–797.

21. Gielen GH, Gessi M, Hammes J, Kramm CM, Waha A, Pietsch T (2013). H3F3A K27M mutation in pediatric CNS tumors: a marker for diffuse high-grade astrocytomas. Am J Clin Pathol 139:345–349.

22. Gilbertson R J (2011). Finding the perfect partner for medulloblastoma prognostication. Journal of Clinical Oncology : Official Journal of the American Society of Clinical Oncology, 29(29), 3841–2. doi:10.1200/JCO.2011.37.5709.

23. Heaphy CM, De Wilde RF, Jiao Y, Klein AP, Edil BH, Shi C, Bettegowda C, Rodriguez FJ, Eberhart CG, Hebbar S, Offerhaus GJ, McLendon R, Rasheed BA, He Y, Yan H, Bigner DD, Oba- Shinjo SM, Marie SK, Riggins GJ, Kinzler KW, Vogelstein B, Hruban RH, Maitra A, Papadopoulos N, Meeker AK (2011). Altered telomeres in tumors with ATRX and DAXX mutations. Science 333(6041):425. doi: 10.1126/science.1207313.

24. Heaphy CM, Subhawong AP, Hong SM, Goggins MG, Montgomery EA, Gabrielson E, Netto GJ, Epstein JI, Lotan TL, Westra WH, Shih Ie M, Iacobuzio-Donahue CA, Maitra A, Li QK, Eberhart CG, Taube JM, Rakheja D, Kurman RJ, Wu TC, Roden RB, Argani P,DeMarzoAM, Terracciano L, TorbensonM,Meeker AK (2011). Prevalence of the alternative lengthening of telomeres telomere maintenance mechanism in human cancer subtypes. Am J Pathol 179:1608–1615. doi: 10.1016/j.ajpath.2011.06.018.

25. Henson JD, Hannay JA, McCarthy SW, Royds JA, Yeager TR, Robinson RA, Wharton SB, Jellinek DA, Arbuckle SM, Yoo J, Robinson BG, Learoyd DL, Stalley PD, Bonar SF, Yu D, Pollock RE, Reddel RR (2005). A robust assay for alternative lengthening of telomeres in tumors shows the significance of alternative lengthening of telomeres in sarcomas and astrocytomas. Clin Cancer Res Off J Am Assoc Cancer Res 11:217–225.

26. Horn S, Figl A, Rachakonda PS, Fischer C, Sucker A, Gast A, Kadel S, Moll I, Nagore E, Hemminki K, Schadendorf D, Kumar R (2013). TERT promoter mutations in familial and sporadic melanoma. Science 339:959–961.

27. Hovestadt V, Remke M, Kool M, Northcott PA, Fischer R, … Jones DTW (2013). Robust molecular subgrouping and copy-number profiling of medulloblastoma from small amounts of archivial tumour material using high-density DNA methylation arrays. *Acta Neuropathologica 125(6):913-916*. doi: 10.1007/s00401-013-1126-5.

28. Huang DS, Wang Z, He XJ, Diplas BH, Yang R, Killela PJ, Liang J, Meng Q, Ye ZY, Wang W, Jiang XT, Hu L, He XL, Zhao ZS, Xu WJ, Wang HJ, Ma YY, Xia YJ, Li L, Zhang RX, Jin T, Zhao ZK, Xu J, Yu S, Wu F, Wang SZ, Jiao YC, Yan H, Tao HQ (2015). Recurrent *TERT* promoter mutations identified in a large-scale study of multiple tumor types are associated with increased *TERT* expression and telomerase activation. Eur J Cancer.; 51(8): 969–976. doi: 10.1016/j.ejca.2015.03.010.

29. Jiao Y, Killela PJ, Reitman ZJ, Rasheed AB, Heaphy CM, de Wild RF, Rodriguez FJ, Rosemberg S, Oba-Shinjo SM, Nagahashi Marie SK, Bettegowda C, Agrawal N, Lipp E, Pirozzi C, Lopez G, He Y, Friedman H, Friedman AH, Riggins GJ, Holdhoff M, Burger P, McLendon R, Bigner DD, Vogelstein B, Meeker AK, Kinzler KW, Papadopoulos N, Diaz LA, Yan H (2012). Frequent ATRX, CIC, FUBP1 and IDH1 mutations refine the classification of malignant gliomas. Oncotarget 3:709–722.

30. Karremann M, Rausche U, Roth D, Kuhn A, Pietsch T, Gielen GH, Warmuth-Metz M, Kortmann RD, Straeter R, Gnekow A, Wolff JE, Kramm CM (2013). Cerebellar location may predict an unfavourable prognosis in paediatric high-grade glioma. Br J Cancer 109:844–851.

31. Killela PJ, Reitman ZJ, Jiao Y, Bettegowda C, Agrawal N, Diaz LAJr, FriedmanAH, Friedman H, Gallia GL, Giovanella BC, GrollmanAP, He TC, He Y, Hruban RH, Jallo GI, Mandahl N, Meeker AK, Mertens F, Netto GJ, Rasheed BA, Riggins GJ, Rosenquist TA,Schiffman M, Shih Ie M, Theodorescu D, Torbenson MS,Velculescu VE, Wang TL, Wentzensen N, Wood LD, Zhang M, McLendon RE, Bigner DD, Kinzler KW, Vogelstein B, Papadopoulos N, Yan H (2013). TERT promoter mutations occur frequently in gliomas and a subset of tumors derived from cells with low rates of self-renewal. Proc Natl Acad Sci USA 110:6021–6026.

32. Kim J-H, Huse JT, Huang Y, Lyden D, Greenfield JP (2013). Molecular diagnostics in paediatric glial tumours. Lancet Oncol 14:19.

33. Koelsche C, Sahm F, Capper D, Reuss D, Sturm D, Jones DTW, Kool M, Northcott PA, Wiestler B, Bohmer K, Meyer J, Marwin C, Hartmann C, Mittelbronn M, Platten M, Brokinkel B, Seiz M, Herold-Mende C, Unterberg A, Schittenhelm J, Weller M, Pfister S, Wick W, Korshunov A, von Deimling A (2013). Distribution of TERT promoter mutations in pediatric and adult tumors of the nervous system. Acta Neuropathol 126:907–914.

34. Koelsche C, Vinagre J, Almeida A, Populo H, Batista R, Lyra J, Pinto V, Coelho R, Celestino R, Prazeres H, Lima L, Melo M, da Rocha AG, Preto A, Castro P, Castro L, Pardal F, Lopes JM, Santos LL, Reis RM, Cameselle-Teijeiro J, Sobrinho-Simoes M,

Lima J, Maximo V, Soares P (2013). Frequency of TERT promoter mutations in human cancers. Nat Commun 4:2185.

35. Kool M, Koster J, Bunt J, Hasselt NE, Lakeman A, van Sluis P, Troost D, Schouten-van Meeteren N, Caron HB, Cloos J, Mrsic A, Ylstra B, Grajkowska W, Hartmann W, Pietsch T, Ellison D, Clifford SC, Versteeg R (2008). Integrated genomics identifies five medullo-blastoma subtypes with distinct genetic profiles, pathway signatures and clinicopathological features. PLoS one 3(8): e3088.

36. Kool M, Korshunov A, Remke M, Jones DTW, Schlanstein M, Northcott PA, … Pfister SM (2012). Molecular subgroups of medulloblastoma: an international meta-analysis of transcriptome, genetic aberrations, and clinical data of WNT, SHH, Group 3, and Group 4 medulloblastomas. Acta Neuropathologica, 123(4), 473–84. doi:10.1007/s00401-012-0958-8.

37. Korshunov A, Remke M, Kool M, Hielscher T, Northcott PA, Williamson D, … Pfister SM (2012). Biological and clinical heterogeneity of MYCN-amplified medulloblastoma. Acta Neuropathologica, 123(4), 515–27. doi:10.1007/s00401-011-0918-8.

38. Lamont JM, Mcmanamy CS, Pearson AD, Clifford SC, & Ellison DW (2004). Combined Histopathological and Molecular Cytogenetic Stratification of Medulloblastoma Patients. Clinical Cancer Research, 5482–5493.

39. Lannering B, Rutkowski S, Doz F, Pizer B, Gustafsson G, Navajas A et al (2012). Hyperfractionated versus conventional radiotherapy followed by chemotherapy in standard-risk medulloblastoma: results from the randomized multicenter HITSIOP PNET 4 trial. J Clin Oncol 30:3187–3193. doi:10.1200/jco.2011.39.8719.

40. Legoix P, Bluteau O, Bayer J, Perret C, Balabaud C, Belghiti J, … Zucman-Rossi J (1999). Beta-catenin mutations in hepatocellular carcinoma correlate with a low rate of loss of heterozygosity. Oncogene, 18(27), 4044–6. doi:10.1038/sj.onc.1202800.

41. Liu XY, Gerges N, Korshunov A, Sabha N, Khuong-Quang DA, Fontebasso AM, Fleming A, Hadjadj D, Schwartzentruber J, Majewski J, Dong Z, Siegel P, Albrecht S, Croul S, Jones DT, Kool M, Tonjes M, Reifenberger G, Faury D, Zadeh G, Pfister S, Jabado N (2012). Frequent ATRX mutations and loss of expression in adult diffuse astrocytic tumors carrying IDH1/IDH2 and TP53 mutations. Acta Neuropathol 124:615–625.

42. Louis DN, Ohgaki H, Wiestler OD, Cavenee WK. WHO Classification of tumours of the central nervous system. Lyon, IARC 2007.

43. Lovejoy CA, Li W, Reisenweber S, Thongthip S, Bruno J, de Lange T, De S, Petrini JHJ, Sung PA, Jasin M, Rosenbluh J, Zwang Y, Weir BA, Hatton C, Invanova E, Macconalli L, Hanna M, Hahn WC, Lue NF, Reddel RR, Jiao Y, Kinzler K, Vogelstein B, Papdopoulos N, Meeker A (2012). Loss of ATRX, genome instability, and an altered

DNA damage response are Hallmarks of the alternative lengthening of telomeres pathway. PloS Genet.8.

44. Mack SC, Witt H, Piro RM, Gu L, Zuyderduyn S, Stutz AM, Wang X, Gallo M, Garzia L, Zayne K, Zhang X, Ramaswamy V, Jager N, Jones DTW, Sill M, Pugh TJ, Ryzhova M, Wani KM, Shih DJH, Head R, Remke M, Bailey SD, Zichner T, Faria CC, Barszczyk M, Stark S, Seker-Cin H, Hutter S, Johann P, Bender S et al (2014). Epigenomic alterations define lethal CIMP-positive ependymomas of infancy. Nature 506:445–450.

45. Mangerel J, Price A, Castelo-Branco P, Brzezinski J, Buczkowicz P, Rakopoulos P, Merino D, Baskin B, Wasserman J, Mistry M, Barszczyk M, Picard D, Mack S, Remke M, Starkman H, Elizabeth C, Zhang C, Alon N, Lees J, Andrulis IL, Wunder JS, Jabado N, Johnston DL, Rutka JT, Dirks PB, Bouffet E, Taylor MD, Huang A, Malkin D, Hawkins C, Tabori U (2014) Alternative lengthening of telomeres is enriched in, and impacts survival of *TP53* mutant pediatric malignant brain tumors. Acta Neuropathol 128:853–862. doi 10.1007/s00401-014-1348-1.

46. Marian CO, Cho SK, McEllin BM, Maher EA, Hatanpaa KJ, Madden CJ, Mickey BE, Wright WE, Shay JW, Bachoo RM (2010). The telomerase antagonist, imetelstat, efficiently targets glioblastoma tumor-initiating cells leading to decreased proliferation and tumor growth. Clin Cancer Res 16(1):154–163.

47. Merchant TE, Pollack IF, Loeffler JS (2010). Brain tumors across the age spectrum: biology, therapy, and late effects. Semin Radiat Oncol 20:58–66.

48. Montanaro L, Calienni M, Ceccarelli C, Santini D, Taffurelli M, Pileri S, Trere D, Derenzini M (2008). Relationship between dyskerin expression and telomerase activity in human breast cancer.Cell Oncol Off J Int Soc Cell Oncol 30:483–490.

49. Massimino M, Giangaspero F, Garrè ML, Gandola L, Poggi G, Biassoni V, Gatta G, Rutkowski S (2011). Childhood medullobastoma. *Critical Reviews in Oncology/Hematology 79* 65–83.

50. Nabetani A, Ishikawa F (2011). Alternative lengthening of telomeres pathway: recombination-mediated telomere maintenance mechanism in human cells. J Biol Chem 149:5-14.

51. Nandakumar J, Cech TR (2013). Finding the end: recruitment of telomerase to telomeres. Nat Rev Mol Cell Biol 14:69–82.

52. Nonoguchi N, Ohta T, Oh JE, Kim YH, Kleihues P, Ohgaki H (2013). TERT promoter mutations in primary and secondary glioblastomas. Acta Neuropathol 126:931–937.

53. Northcott PA, Korshunov A, Witt H, Hielscher T, Eberhart CG, Mack S, Taylor MD (2011). Medulloblastoma comprises four distinct molecular variants. J Clin Oncol 29(11):1408–1414.

54. Northcott PA, Shih DJH, Peacock J, Garzia L, Morrissy S, Zichner T, … Taylor MD (2012a). Subgroup-specific structural variation across 1,000 medulloblastoma genomes. Nature, 488(7409), 49–56. doi:10.1038/nature11327.

55. Northcott PA, Shih DJH, Remke M, Cho YJ, Kool M, Hawkins C, … Taylor MD (2012b). Rapid, reliable, and reproducible molecular sub-grouping of clinical medulloblastoma samples. Acta Neuropathologica, 123(4), 615–26. doi:10.1007/s00401-011-0899-7.

56. Noushmehr H, Weisenberger DJ, Diefes K, Phillips HS, Pujara K, Bergman BP, Pan F, Pelloskj CE, Sulman EP, Bhat KP, Verhaan RG, Hoadley KA, Hayes DN, Perou CM, Schmidt HK, Ding L, Wilson RK, Van Der Berg D, Shen H, Bengtsson H, Neuvial P, Cope LM, Buckley J, Herman JG, Baylin SB, Laird PW, Aldape K (2010). Identification of a CpG island methylator phenotype that defines a distinct subgroup of glioma. Cancer Cell 17(5):510-22. doi: 10.1016/j.ccr.2010.03.017.

57. Oganasian L, Karlseder J (2009). Telomeric armor: the layers of end protection. J Cell Sci 122:4013–4025.

58. Parker M, Mohankumar KM, Punchihewa C, Weinlich R, Dalton JD, Li Y, Lee R, Tatevossian RG, Phoenix TM, Thiruvenkatam R, White E, Tang B, Orisme W, Gupta K, Rusch M, Chen X, Li Y, Nagahawhatte P, Hedlund E, Finkelstein D, Wu G, Shurtleff S, Easton J, Boggs K, Yergeau D, Vadodaria B, Mulder HL, Becksfort J, Gupta P, Huether R et al (2014). C11orf95-RELA fusions drive oncogenic NF-κB signalling in ependymoma. Nature 506:451–455.

59. Paugh BS, Qu C, Jones C, Liu Z, Adamowicz-Brice M, Zhang J, Bax DA, Coyle B, Barrow J, Hargrave D, Lowe J, Gajjar A, Zhao W, Broniscer A, Ellison DW, Grundy RG, Baker SJ (2010). Integrated molecular genetic profiling of pediatric high-grade gliomas reveals key differences with the adult disease. J Clin Oncol 28:3061–3068.

60. Ramaswamy V, Remke M, Bouffet E, Faria CC, Perreault S, Cho YJ, … Taylor MD (2013). Recurrence patterns across medulloblastoma subgroups: an integrated clinical and molecular analysis. The Lancet Oncology, 14(12), 1200–7. doi:10.1016/S1470-2045(13)70449-2.

61. Ramaswamy V, Remke M, Bouffet E, Bailey S, Clifford SC, Doz F, Kool M, Dufour C, Vassal G, Milde T, Witt O, · Von Hoff K, Pietsch T, Northcott PA, Gajjar A, Robinson GW, Padovani L, André N, Massimino M, Pizer B, Packer R, Rutkowski S, Pfister SM, Taylor MD, Pomeroy SL (2016). Risk stratification of childhood medulloblastoma in the molecular era: the current consensus. Acta Neuropathol 131:821–831. doi 10.1007/s00401-016-1569-6.

62. Reifenberger G, Weber RG, Riehmer V, Kaulich K, Willscher E, Wirth H, Gietzelt J, Hentschel B, Westphal M, Simon M, Schackert G, Schramm J, Matschke J, Sabel MC, Gramatzki D, Felsberg J, Hartmann C, Steinbach JP, Schlegel U, Wick W, Radlwimmer

B, Pietsch T, Tonn JC, Von Deimling A, Binder H, Weller M, Loeffler M; German Glioma Network (2014). Molecular characterization of long-term survivors of glioblastoma using genome- and transcriptome-wide profiling. Int J Cancer 135(8):1822-31.

63. Remke M, Hielscher T, Korshunov A, Northcott PA, Bender S, Kool M, … Pfister SM (2011a). FSTL5 is a marker of poor prognosis in non-WNT/non-SHH medulloblastoma. Journal of Clinical Oncology : Official Journal of the American Society of Clinical Oncology, 29(29), 3852–61. doi:10.1200/JCO.2011.36.2798.

64. Remke M, Hielscher T, Northcott PA, Witt H, Ryzhova M, Wittmann A, … Korshunov A (2011b). Adult medulloblastoma comprises three major molecular variants. Journal of Clinical Oncology : Official Journal of the American Society of Clinical Oncology, 29(19), 2717–23. doi:10.1200/JCO.2011.34.9373.

65. Remke M, Ramaswamy V, Peackock J, Shih DJH, Koelsche C, Northcott PA, Hill N, Cavalli FMG, Kool M, Wang X, Mack SC, Barszczyk M, Morissi AS, Wu X, Agnihotri S, Luu B, Jones DTW, Garzia L, Dubuc AM, Zhukova N, Vanner R, Kros JM, French PJ, Van Meir EG, Vibhakar R, Zitterbart K, Chan JA, Bognar L, Kekner A, Lach B et al (2013). TERT promoter mutations are highly recurrent in SHH subgroup medulloblastoma. Acta Neuropathol 126:917–929.

66. Robinson G, Parker M, Kranenburg TA, Lu C, Chen X, Ding L, … Gilbertson RJ (2012). Novel mutations target distinct subgroups of medulloblastoma. Nature, 488(7409), 43–8. doi:10.1038/nature11213.

67. Rubtsova MP, Vasilkova DP, Malyavko AN, Naraikina YV, Zvereva MI, Dontsova OA (2012). Telomere lengthening and other functions of telomerase. Acta Naturae 2:44–61.

68. Schwartzentruber J, Korshunov A, Liu XY, Jones DT, Pfaff E, Jacob K, Sturm D, Fontebasso AM, Quang DA, Tonjes M, Hovestadt V, Albercht S, Kool M, Nantel A, Konermann C, Lindroth A, Jager N, Rausch T, Ryzhova M, Korbel JO, Hielscher T, Hauser P, Garami M, Klekner A, Bognar L, Ebinger M, Schuhmann MU, Scheurlen W, Pekrun A, Fuhwald MC et al (2012). Driver mutations in histone H3.3 and chromatin remodelling genes in paediatric glioblastoma. Nature 482:226–231. doi:10.1038/nature10833.

69. Shih DJ, Northcott PA, Remke M, Korshunov A, Ramaswamy V, Kool M et al (2014). Cytogenetic prognostication within medulloblastoma subgroups. J Clin Oncol 32:886–896. doi:10.1200/jco.2013.50.9539.

70. Sturm D, Witt H, Hovestadt V, Khuong-Quang DA, Jones DT, Konermann C, Pfaff E, Tonjes M, Sill M, Bender S, Kool M, Zapatka M, Becker N, Zucknick M, Hielscher T, Liu XY, Fontebasso AM, Ryzhova M, Albrecht S, Jacob K, Wolter M, Ebinger M, Schuhmann MU, van Meter T, Fruhwald MC, Hauch H, Pekrun A, Radlwimmer B, Niehues T, von Komorowski G, Durken M, Kulozik AE, Madden J, Donson A, Foreman

NK, Drissi R, Fouladi M, Scheurlen W, von Deimling A, Monoranu C, Roggendorf W, Herold-Mende C, Unterberg A, Kramm CM, Felsberg J, Hartmann C, Wiestler B,Wick W, Milde T, Witt O, Lindroth AM, Schwartzentruber J, Faury D, Fleming A, Zakrzewska M, Liberski PP, Zakrzewski K, Hauser P, Garami M, Klekner A, Bognar L, Morrissy S, Cavalli F, Taylor MD, van Sluis P, Koster J, Versteeg R, Volckmann R, Mikkelsen T, Aldape K, Reifenberger G, Collins VP, Majewski J, Korshunov A, Lichter P, Plass C, Jabado N, Pfister SM (2012). Hotspot mutations in H3F3A and IDH1 define distinct epigenetic and biological subgroups of glioblastoma. Cancer Cell 22:425–437.

71. Tharmalingam S and Hampson DR (2016). The Calcium-Sensing Receptor and Integrins in Cellular Differentiation and Migration. Front Physiol. 2016; 7: 190. doi: 10.3389/fphys.2016.00190.

72. Taylor MD, Northcott PA, Korshunov A, Remke M, Cho YJ, Clifford SC, Eberhart CG, Parsons DW, Rutkowski S, Gajjar A, Ellison DW, Lichter P, Gilbertson RJ, Pomeroy SL, Kool M, Pfister SM (2012). Molecular subgroups of medulloblastoma: the current consensus. Acta Neuropathol 123(4), 465–72. doi:10.1007/s00401-011-0922-z.

73. Van Bueren AO, Kortmann RD, Von Hoff K, Friedrich C, Mynarek M, Muller K, Goschzik T, Mühlen A, Gerber N, Warmuth-Metz M, Soerensen N, Deinlein F, Benesch M, Zwiener I, Kwiecien R, Faldum A, Bode U, Fleischhack G, Hovestadt V, Kool M, Jones D, Northcott P, Kuehl J, Pfister S, Pietsch T, Rutkowki S (2016). Treatment of Children and Adolescents with Metastatic Medulloblastoma and Prognostic Relevance of Clinical and Biologic Parameters. J Clin Oncol 34(34):4151-4160.

74. Wu X, Northcott PA, Dubuc A, Dupuy AJ, Shih DJ, Witt H et al (2012). Clonal selection drives genetic divergence of metastatic medulloblastoma. Nature 482:529–533. doi:10.1038/nature10825.

75. Yang H, Zhang Q, He J and Lu W (2010). Regulation of calcium signaling in lung cancer. J Thorac Dis. 2010 Mar; 2(1): 52–56.

76. Yih-Fung Chen, Ying-Ting Chen, Wen-Tai Chiu and Meng-Ru Shen (2013). Remodeling of calcium signaling in tumor progression. Journal of Biomedical Science 2013, 20:23.

77. Zhang D, Ma X, Sun W, Cui P, Zheng Lu (2015). Down-regulated FSTL5 promotes cell proliferation and survival by affecting Wnt/β-catenin signaling in hepatocellular carcinoma. Int J Clin Exp Pathol 2015;8(3):3386-3394.